Molecular Biology of the Cell
Vol. 15, 3196–3209, July 2004

Soi3p/Rav1p Functions at the Early Endosome to Regulate Endocytic Trafficking to the Vacuole and Localization of *Trans*-Golgi Network Transmembrane Proteins

György Sipos,*†‡ Jason H. Brickner,*†§ E.J. Brace,* Linyi Chen,‖¶ Alain Rambourg,# Francois Kepes,#@ and Robert S. Fuller* **

*Department of Biological Chemistry, University of Michigan Medical Center, Ann Arbor, Michigan 48109-0606; ‖Department of Pharmacology, Wayne State University School of Medicine, Detroit, Michigan 48201, and #Departement de Biologie Cellulaire et Moleculaire, Commissariat á l'Energie Atomique Saclay, Gif-sur-Yvette 91191 Cedex, France

Submitted October 22, 2003; Revised April 5, 2004; Accepted April 7, 2004
Monitoring Editor: Randy Schekman

***SOI3* was identified by a mutation, *soi3-1*, that suppressed a mutant *trans*-Golgi network (TGN) localization signal in the Kex2p cytosolic tail. *SOI3*, identical to *RAV1*, encodes a protein important for regulated assembly of vacuolar ATPase. Here, we show that Soi3/Rav1p is required for transport between the early endosome and the late endosome/prevacuolar compartment (PVC). By electron microscopy, *soi3-1* mutants massively accumulated structures that resembled early endosomes. *soi3*Δ mutants exhibited a kinetic delay in transfer of the endocytic tracer dye FM4-64, from the 14°C endocytic intermediate to the vacuole. The *soi3*Δ mutation delayed vacuolar degradation but not internalization of the a-factor receptor Ste3p. By density gradient fractionation, Soi3/Rav1p associated as a peripheral protein with membranes of a density characteristic of early endosomes. The *soi3* null mutation markedly reduced the rate of Kex2p transport from the TGN to the PVC but had no effect on vacuolar protein sorting or cycling of Vps10p. These results suggest that assembly of vacuolar ATPase at the early endosome is required for transport of both Ste3p and Kex2p from the early endosome to the PVC and support a model in which cycling through the early endosome is part of the normal itinerary of Kex2p and other TGN-resident proteins.**

INTRODUCTION

Steady-state localization of *trans*-Golgi network (TGN) membrane proteins in the budding yeast *Saccharomyces cerevisiae* is achieved by continuous cycles of vesicular transport between the TGN and post-TGN compartments such as the late endosome or prevacuolar compartment (PVC) (Fuller *et al*., 1988; Vida *et al*., 1993; Cereghino *et al*., 1995; Brickner and Fuller, 1997; Bryant and Stevens, 1997). Kex2p and Ste13p, proteolytic processing enzymes involved in maturation of α-mating factor and other substrates (Fuller *et al*., 1988), are localized to the TGN by the function of TGN localization signals (TLSs) in their cytosolic tails (C-tails) (Brickner and Fuller, 1997; Bryant and Stevens, 1997). TLS1 directs retrieval from the PVC to the TGN and consists of two essential aromatic residues separated by a nonessential charged or polar residue ($Tyr_{713}Glu_{714}Phe_{715}$ for Kex2p and $Phe_{85}Gln_{86}Phe_{87}$ for Ste13p) (Wilcox *et al*., 1992; Nothwehr *et al*., 1993; Redding *et al*., 1996a). Substitutions for Tyr_{713} in the TLS1 of Kex2p leads to loss of TGN localization and rapid delivery of the protein to the vacuole (Wilcox *et al*., 1992; Redding *et al*., 1996a). A less well defined signal, TLS2, requires sequences distal to TLS1 in the Kex2p C-tail and functions to delay transport of Kex2p from the TGN to the PVC, possibly by promoting TGN retention (Brickner and Fuller, 1997). A signal similar to TLS2 is found in the Ste13p C-tail (Bryant and Stevens, 1997).

Using a mating assay sensitive to the efficiency of α-factor processing by Kex2p, we isolated allele-specific mutant suppressors *soi1*, *SOI2*, and *soi3* that suppressed the effects of a TLS1 point mutation ($Y_{713}A$) in Kex2p but not of a deletion of TLS1 or of the entire C-tail (Redding *et al*., 1996a). These *soi* mutations also suppressed effects of point mutations in the Ste13p TLS1 signal (Redding *et al*., 1996a). Cloning of *SOI1*, allelic to *VPS13*, revealed that this gene encoded a novel 350-kDa peripheral membrane protein whose human homologues include two disease loci (Brickner and Fuller, 1997; Rampoldi *et al*., 2001; Ueno *et al*., 2001; Kolehmainen *et al*., 2003). Suppression of the mislocalization of $Y_{713}A$ Kex2p by a *soi1* mutation required TLS2, indicating that TLS2 function became activated in the absence of Soi1p, slowing the

Article published online ahead of print. Mol. Biol. Cell 10.1091/mbc.E03–10–0755. Article and publication date are available at www.molbiolcell.org/cgi/doi/10.1091/mbc.E03–10–0755.

† These authors made comparable contributions to this work.

Present addresses: ‡Department of Medical Biochemistry, University and Biocenter of Vienna, A-1030 Vienna, Austria; §Department of Biochemistry and Biophysics, University of California, San Francisco, CA 94143; ¶Department of Molecular and Integrative Physiology, University of Michigan Medical Center, Ann Arbor, MI 48109-0622; @ Dynamique de la Compartimentation Cellulaire, Institut des Sciences du Végétal, Centre National de la Recherche Scientifique Unité Propre de Recherche 2355, Gif-sur-Yvette, France, and Epigenomics Project/Genopole, Evry, France.

** Corresponding author. E-mail address: bfuller@umich.edu.

Abbreviations used: ALP, alkaline phosphatase; API, aminopeptidase I; C-tail, cytosolic tail; GFP, green fluorescent protein; HA, hemagglutinin epitope; IP, immunoprecipitation; PVC, prevacuolar compartment; TLS, *trans*-Golgi network localization signal; Vps, vacuolar protein sorting.

escape of Kex2p from the TGN (Brickner and Fuller, 1997). The *soi1* mutants also displayed defective TLS1-dependent localization, resulting in aberrant localization not only of Kex2p but also of the vacuolar precursor sorting receptor Vps10p and of A-ALP, a hybrid protein in which the Ste13p C-tail is fused to alkaline phosphatase (ALP). These results indicated that Soi1p acts both at the PVC to stimulate TLS1 function and at the TGN to repress TLS2 function and consequently facilitates cycling of transmembrane proteins between the TGN and PVC (Brickner and Fuller, 1997).

Transport of Kex2p from the TGN to the PVC requires clathrin and the dynamin homolog Vps1p (Seeger and Payne, 1992; Wilsbach and Payne, 1993; Nothwehr *et al*., 1995; Redding *et al*., 1996a,b). Mutations in two types of clathrin adaptors affect Kex2p localization. These are the Gga proteins, encoded by *GGA1* and *GGA2*, and the Adaptor Protein (AP)-1 adaptor complex (Black and Pelham, 2001). Mutations in the *GGA* genes blocked transport of carboxypeptidase Y (CPY) to the vacuole, abrogated TGN to PVC transport of Vps10p and Pep12p, and altered the efficiency of pro-α-factor processing by Kex2p (Black and Pelham, 2000; Dell'Angelica *et al*., 2000; Hirst *et al*., 2000; Costaguta *et al*., 2001). Effects of mutations in genes encoding AP-1 subunits are only seen in combination with either *gga* mutations or clathrin mutations (Phan *et al*., 1994; Stepp *et al*., 1995; Huang *et al*., 1999; Yeung *et al*., 1999), suggesting that the transport pathway governed by AP-1 is either less important for Kex2p localization or is redundant with other pathways. Recently, it has been suggested that AP-1 adaptors function in transport between the TGN and early endosome of Kex2p, Ste13p, and chitin synthase III (Chs3p), suggesting that TGN membrane proteins such as Kex2p and Ste13p access the early endosome (Valdivia *et al*., 2002; Ha *et al*., 2003).

Here, we have cloned the *SOI3* gene, which we find to be identical to *RAV1*. Rav1p was isolated as a Skp1p-interacting protein that is part of a complex that contains Rav2p and the V_1 subcomplex of the proton-translocating vacuolar ATPase (V-ATPase) (Seol *et al*., 2001; Smardon *et al*., 2002). Both *RAV1* and *RAV2* were shown to be important for glucose-regulated assembly of V_1 onto V_0 to form functional V-ATPase on the vacuolar membrane (Seol *et al*., 2001). Analysis of the effects of *soi3* mutations demonstrates that loss of Soi3p function results both in alterations in the localization of TGN membrane proteins as well as selective defects in delivery of endocytic cargo to the vacuole. A synthesis of these results suggests that assembly of vacuolar ATPase at the early endosome in yeast is essential for early endosome maturation and efficient transport from the early endosome to the PVC.

MATERIALS AND METHODS

Antibodies and Reagents

Antisera against the Kex2 Ctail and lumenal domains were as described previously (Wilcox and Fuller, 1991; Wilcox *et al*., 1992). Anti-Pep12 and anti-CPY monoclonal antibodies were from Molecular Probes (Eugene, OR). Anti-hemagglutinin (HA) monoclonal antibody 12CA5 was from Roche Diagnostics (Indianapolis, IN). Antisera against Anp1p, Mnn1p, Chs3p, Pep12p, Vps10p, CPY, ALP, aminopeptidase I (API), and Ste3p were gifts of Drs. S. Munro (Medical Research Council, Cambridge, United Kingdom), T. Graham (Vanderbilt University, Nashville, TN), R. Schekman (University of California, Berkeley, CA), S. Emr (University of California, San Diego, CA), D. Klionsky (University of Michigan, Ann Arbor, MI), and N. Davis (Wayne State University, Detroit, MI). Antibodies against Ste3p were affinity purified as described previously (Redding *et al*., 1991; Roth *et al*., 1998). Rabbit anti-mouse IgG was from Jackson ImmunoResearch Laboratories (West Grove, PA), and horseradish peroxidase-conjugated secondary antibodies were from Amersham Biosciences (Piscataway, NJ). Boc-Leu-Lys-Arg-7-amino-4-methylcoumarin (LKR-AMC) was from Bachem Biosciences (King of Prussia, PA). Restriction and DNA modification enzymes were from New England Biolabs (Beverly, MA). Unless indicated otherwise, all other chemicals and reagents were from Sigma-Aldrich (St. Louis, MO).

Strains and Plasmids

Plasmids containing *KEX2* under the *KEX2* promoter on yeast centromere plasmids were pCWKX10 (wild-type Kex2p), pCWKX11 (Y_{713}A-Kex2p), and pCWKX10-I718tail (I718tail-Kex2p) (Wilcox *et al*., 1992; Redding *et al*., 1996a; Brickner and Fuller, 1997). Plasmids containing *KEX2* under the *GAL1* promoter on yeast centromere plasmids were pCWKX20 (wild type), pCWKX21 (Y_{713}A-Kex2p), pCWKX27 (C-tailΔ-Kex2p), pCWKX20-I718tail (I718tail-Kex2p), and pCWKX21-I718tail (Y_{713}A, I718tail-Kex2p) (Wilcox *et al*., 1992; Redding *et al*., 1996a; Brickner and Fuller, 1997). Plasmids pRS303-*SOI3*.1 and pRS313-*SOI3* were constructed by ligating an *Eco*RI fragment containing base pairs 491021–498250 from yeast chromosome X into pRS303 (*HIS3* integrating plasmid) and pRS313 (*HIS3 CEN ARS* plasmid), respectively (Sikorski and Hieter, 1989). Plasmid p*SOI3-HA* was generated from pRS313-*SOI3*.1 by mutating the final three codons of *SOI3* from GAC TTT GTA to GGC GGC CGC by polymerase chain reaction (PCR) to generate a *Not*I site and ligating a fragment encoding a triple HA epitope tag (Tyers *et al*., 1992). Plasmid p413ADH-*SOI3* was constructed by PCR amplifying the *SOI3* structural gene and ligating the resulting fragment into the *Eco*RI site of p413ADH (Mumberg et al., 1995). To express a Soi3p fusion to green fluorescent protein (GFP), p*SOI3*-GFP was created by ligating the 0.75-kb *Not*I fragment of pSF-GP1 (gift of Jeanne Hirsch, Mt. Sinai School of Medicine, New York, NY) into the *Not*I site of pRS313-*SOI3*.1. Plasmids p*SOI3*-GFP-SL and p*SOI3-HA*-SL were created by replacing the *Sac*I sites in p*SOI3*-GFP and p*SOI3-HA* with a *Sal*I site by linker ligation. Plasmids p413ADH-*SOI3*-GFP and p413ADH-*SOI3-HA* were created by ligating the *Nar*I/*Sal*I fragments of p*SOI3*-GFP-SL and p*SOI3-HA*-SL containing the C termini of *SOI3*-GFP and *SOI3-HA*, into p413ADH-*SOI3* cleaved by *Nar*I plus *Sal*I. Expression of Soi3-Soi3-GFP fully complemented the *soi3* null mutation (our unpublished data).

Strains used in this study, created by standard genetic crosses and/or by transformation, are shown in Table 1. Yeast media were as described (Rose *et al*., 1990). Two-step gene replacements were used to convert *STE3* either to *Gal1-STE3*, *Gal1-STE3-HA* or to *Gal1-STE3Δ365*, as described previously (Roth and Davis, 1996; Chen and Davis, 2002). To delete *VPS1*, the complete coding sequence of *VPS1* was replaced with *Kluyveromyces lactis LEU2* as described previously (Gueldener *et al*., 2002). The *vps1-100-ts* allele was introduced by transplacement. Plasmid pCAV40 (generous gift of Tom Stevens, University of Oregon, Portland, OR) containing *vps1-100-ts* was digested with *Eco*RI, transformed into CRY1, and Ura^+ transformants were selected. Ura^- recombinants isolated by 5-fluoroorotic acid selection were tested by the CPY colony blot assay to identify a strain carrying the *vps1-100-ts* allele (EBY73).

Cloning and Analysis of SOI3

Strain SPB400-3D carrying plasmid pCWKX10 was transformed with the *CEN ARS LEU2* genomic library YPH1 (ATCC no. 77162). Library transformants were screened by replica-plating to both YPD + 6 mM $ZnCl_2$ and YPD + 10 mM $ZnCl_2$. Zinc-resistant transformants were tested for plasmid dependence and for their ability to complement the Soi^+ phenotype measured by the onset of impotence experiment as described previously (Redding *et al*., 1996a). Two independent transformants displayed plasmid-dependent complementation of both the Zn^{2+} sensitivity and the Soi^+ phenotype (Redding *et al*., 1996a). DNA sequencing revealed that the inserts corresponded to base pairs 491021–498727 on chromosome X. To determine whether this DNA region corresponded to *SOI3*, an *Eco*RI fragment corresponding to base pairs 491021–498250 from chromosome X was cloned into pRS303 (*HIS3* integrating plasmid) (Sikorski and Hieter, 1989) to create pRS303-SOI3.1A. This plasmid was linearized with *Stu*I, transformed into KRY18-1B, and His^+ transformants were crossed to SPB400-3D transformed with pKWKX21. The resulting diploid was sporulated and analyzed by random spore analysis, demonstrating linkage of the integrated marker and *soi3-1* (46 *MATαMATα* strains: 0 Soi^+ His^+, 12 Soi^+ His^-, 32 Soi^- His^+, and 0 Soi^- His^-), also confirmed by tetrad analysis (our unpublished data). DNA sequence analysis of the inserts combined with examination of the published yeast genomic sequence showed that only two full-length open reading frames, YJR033c and *PET191*, were contained within the overlapping region. YJR033c was seen as the more likely candidate, because *soi3-1* strains grew on nonfermentable carbon sources (our unpublished data). However, subclones containing YJR033c along with 232 base pairs of the 5′ untranslated region and 220 base pairs of *PET191* did not fully complement both the Zn^{2+} sensitivity and suppressor phenotypes (our unpublished data). To confirm that expression of YJR033c alone complemented *soi3-1* phenotypes, YJR033c was amplified by PCR and subcloned under the control of the *ADH* promoter on a single copy *CEN* plasmid (Mumberg *et al*., 1995), resulting in plasmid pADH-YJR033c.

Heterozygous replacement of the complete coding sequence of the *SOI3* gene with the *kan*^{r} gene (Wach *et al*., 1994) in diploid strain KRY18 resulted in GSY11, which was sporulated to generate haploid *soi3*Δ strains (Table 1).

Microscopy

For electron microscopy (EM), cells were fixed, stained, and visualized as described previously (Rambourg *et al*., 1993). For FM4-64 uptake experiments, strains GSY11-2A (*soi3*Δ) and GSY11-4D (*SOI3*) were grown in 10 ml of YPD to ~OD_{600} = 0.9, harvested, and resuspended in 500 μl of cold YPD + 40 μM FM4-64 (Molecular Probes). Cells were incubated on ice for 1 h, washed in

Table 1. Strains used in this study

Strain	Relevant genotype	Parental strain
CRY1[a]	*MAT***a** *ade2-1 can1-100 his3-11,15 leu2-3,112 trp1-1 ura3-1*	W303-1A[a]
CRY2[a]	*MATα ade2-1 can1-100 his3-11,15 leu2-3,112 trp1-1 ura3-1*	W303-1B[a]
CRY3[a]	*MAT***a***/MATα*	CRY1 × CRY2
KRY18[b]	*KEX2/kex2Δ::TRP1*	CRY3
GSY11	*soi3Δ/SOI3*	KRY18
KRY18-1A	*MATα kex2Δ::TRP1*	KRY18
KRY18-1B	*MAT***a** *kex2Δ::TRP1*	KRY18
GSY11-1A	*MAT***a** *soi3Δ::kan*^{r}	GSY11
GSY11-2A	*MATα soi3Δ::kan*^{r}	GSY11
GSY11-4D	*MATα SOI3*	GSY11
GSY11-7A	*MATα soi3Δ::kan*^{r} *kex2Δ::TRP1*	GSY11
SPB400-3D[b]	*MATα soi3-1 kex2Δ::TRP1*	KRY18-1A
KRY200-r2[b]	*MATα soi2-3 kex2Δ::TRP1*	KRY18-1A
KRY208-r3[b]	*MATα soi3-1 kex2Δ::TRP1*	KRY18-1A
JBY135-1A	*MATα soi1Δ1::kan*^{r}	JBY135[c]
JBY135-1C	*MATα soi1Δ1::kan*^{r} *kex2Δ::TRP1*	JBY135[c]
JBY142[c]	*MAT***a** *SOI1-HA*	CRY1
GSY19	*MAT***a** *vps10::kan*^{r}	CRY2
GSY32	*MATα GAL1-STE3*	CRY2
GSY34	*MATα GAL1-STE3 soi3Δ::kan*^{r}	GSY11-2A
GSY35	*MATα GAL1-STE3 soi1Δ2::kan*^{r}	JBY154-1D[c]
GSY36	*MATα GAL1-STE3 soi3Δ::kan*^{r} *pep4::LEU2*	GSY34
GSY40	*MATα GAL1-STE3Δ365*	CRY2
GSY41	*MATα GAL1-STE3Δ365 soi3Δ::kan*^{r}	GSY11-2A
GSY51	*MATα ste3Δ::LEU2*	CRY2
EBY22	*MATα soi3Δ::kan*^{r} *kex2Δ::TRP1 vps27Δ::LEU2*	GSY11-7A
EBY68	*MATα vps1Δ::LEU2*	CRY2
EBY69	*MAT***a***/MATα vps1Δ::LEU2/VPS1 soi3Δ::kan*^{r}*/SOI3*	EBY68xGSY11-1A
EBY73	*MAT***a** *vps1-100-ts*	CRY1
EBY17	*MAT***a***/MATα soi3Δ::kan*^{r}*/soi3Δ::kan*^{r}	GSY11-1AxGSY11-2A
EBY76	*MAT***a***/MATα vps1Δ::LEU2/VPS1 soi3Δ::kan*^{r}*/soi3Δ::kan*^{r}	EBY17
EBY77	*MAT***a***/MATα vps1-100ts/VPS1 soi3Δ::kan*^{r}*/SOI3*	EBY73xGSY11-2A
EBY77-4	*MATα vps1-100-ts*	EBY77
EBY77-8	*MATα vps1-100-ts soi3Δ::kan*^{r}	EBY77

[a] Wilcox *et al.* (1992).
[b] Redding *et al.* (1996a).
[c] Brickner and Fuller, 1997.

cold YPD, and resuspended in 1 ml of cold YPD and incubated at 14°C, with shaking. After 40 min at 14°C, 500 μl of cells was harvested and resuspended in 400 μl of prewarmed 30°C YPD. Cells were harvested, washed in 1× 100 μl of 10 mM NaN_3, 0 mM NaF, resuspended in 25 μl of 10 mM NaN_3, 10 mM NaF, and stored on ice until they were examined using an Axioskop microscope (Carl Zeiss, Thornwood, NY), recording data on film as described previously (Brickner and Fuller, 1997). Soi3-GFP images were examined using a Nikon Eclipse 800 microscope and an ORCA2 charge-coupled device (Hamamatsu, Bridgewater, NJ). Cells were grown in log phase in minimal medium at 25°C and mounted in low-temperature agarose. Z-stacks were created using eight 0.25-μm steps. ISEE Software (Inovision, Raleigh, NC) was used for image capture and deconvolution of Z-stacks.

Ste3p and Zrt1-HAp Endocytosis

Constitutive turnover of the Ste3p and the **a**-factor–dependent internalization, recycling, and turnover of Ste3Δ365p were all performed as described previously (Chen and Davis, 2000). Expression of Ste3p and related proteins (Ste3Δ365p and Ste3HAp) was regulated from the *GAL1* promoter (Chen and Davis, 2000). Single HA epitope-tagged Zrt1p (Zrt1-HAp) was expressed from its own promoter on plasmid pMC5-HSET (Gitan *et al*., 1998), a gift of David Eide (University of Missouri, Columbia, MO). To induce Zrt1-HAp in *soi3*Δ cells, *soi3*Δ and control cells were pretreated with 1 mM EDTA for 3 h to induce Zrt1-HAp expression, and internalization was initiated by the addition of 2 mM Zn^{2+}. Cell disruption and sample preparation protocols were as described previously (Davis *et al*., 1993).

Subcellular Fractionation

Fractionation procedures followed published methods (Sipos and Fuller, 2002). Cells were spheroplasted with lyticase, and 200-μl samples equivalent to 50 ml of cells (OD_{600} = 1) were frozen over liquid N_2. For differential centrifugation, spheroplasts were thawed and homogenized, and lysates were centrifuged twice at 500 × *g* for 5 min. The supernatant was centrifuged for 15 min at 13,000 × *g*. The resulting pellet (P13) was washed with buffer and pelleted again for 15 min at 13,000. The medium speed supernatant (S13) was split into three samples. One was adjusted to 1 M NaCl, a second to 1% Triton X-100. These samples were incubated on ice for 20 min and centrifuged in a TLS55 rotor in a TLX centrifuge (Beckman Coulter, Fullerton, CA) at 55,000 rpm (200,000 × *g* at r_{avg}) for 30 min to generate P200 and S200 fractions. Samples equivalent to 1 ml of cells (OD_{600} = 1.0) of the P13, S13, P200, and S200 fractions were fractionated by SDS-PAGE, and the presence of markers were analyzed by immunoblotting.

For sucrose gradient fractionation, 0.5 ml of P200 fraction, equivalent to 200 ml of cells (OD_{600} = 1.0), was loaded on the top of the following sucrose step gradient (from the bottom): 0.5 ml of 60%/2.0 ml of 48%/2.5 ml of 40%/2.5 ml of 36%/2.5 ml of 32%/2.0 ml of 29%. The gradient was centrifuged at 41,000 rpm for 17 h at 4°C by using a Beckman Coulter SW41 rotor. Fractions (250 μl) were collected, and 10- to 15-μl samples from each interface were analyzed by immunoblotting and assayed for Kex2 activity, as described previously (Sipos and Fuller, 2002).

^{35}S Pulse-Chase/Immunoprecipitation

^{35}S Pulse-chase/immunoprecipitation experiments were performed essentially as described previously (Wilcox and Fuller, 1991). Cells were labeled with ^{35}S-labeled amino acids (Express Label; Amersham Biosciences). Five-minute pulses were used for ALP, CPY, and API, and 10-min pulses were used for Kex2p and Vps10p. Pulses were followed by chase with nonradioactive methionine and cysteine at 10 mM, and cell samples removed at various times were subjected to glass-bead lysis under denaturing conditions. Immunoprecipitations (IPs) of Kex2p and Vps10p were carried out twice. Other proteins were subjected to single IPs. IPs used polyclonal antisera and

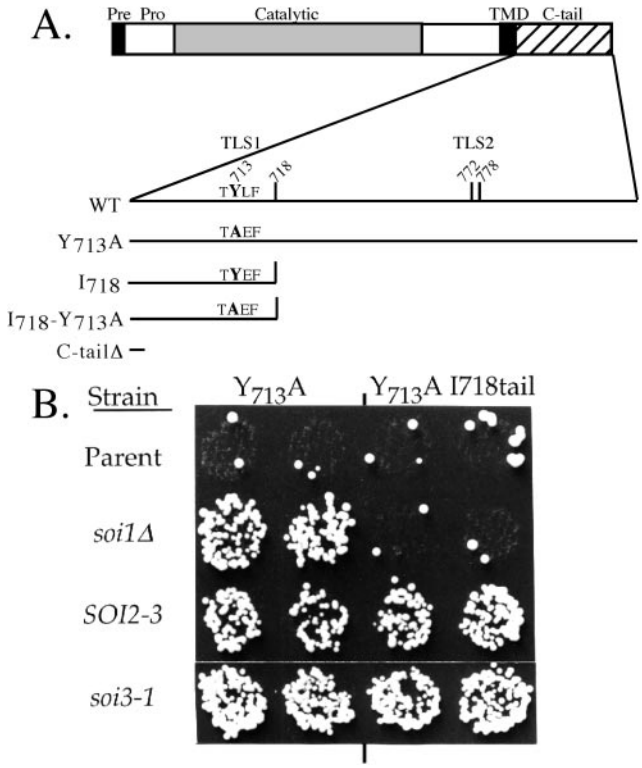

Figure 1. *soi3-1* mutation suppresses a TLS1 mutation in Kex2p in the absence of TLS2. (A) Schematic diagram of Kex2p indicating various C-tail mutants. C-tail ending at 778 is TLS2$^+$; C-tail ending at 772 is TLS2$^-$ (Brickner and Fuller, 1997). (B) *SOI2* and *soi3-1* mutations improve the localization defect of $Y_{713}A$ mutation of Kex2p in the context of both the short (I718tail) and full-length C-tail. KRY18–1A (wild type), JBY135–1C (*soi1*Δ), KRY200-r2 (*SOI2-3*), and KRY208-r3 (*soi3-1*) were transformed either with pCWKX21 (Y_{713}A-Kex2p) or pCWKX21-I718tail (Y_{713}A, I718tail-Kex2p). Cells were shifted from galactose to glucose for 5 h and tested for mating competence (Redding *et al.*, 1996a).

Pansorbin (Calbiochem-Novabichem, La Jolla, CA) (2.5 μl of 50% slurry per equivalent of 1 ml of cells at OD_{600} = 1.0). IPs were fractionated by SDS-PAGE, and radioactive signals were captured and quantified using a PhosphorImager (Amersham Biosciences) and IPLabgel software (Signal Analytics, Vienna, VA). Half-lives were calculated by linear regression.

RESULTS

SOI3 *Corresponds to YJR033c*/RAV1

Unlike *soi1* mutations (Brickner and Fuller, 1997), dominant *SOI2* mutations and the recessive *soi3-1* mutation (Redding *et al.*, 1996a) suppressed the $Y_{713}A$ substitution in TLS1 in the context of a shortened Kex2p C-tail (I718tail) that lacks TLS2 (Figure 1). Neither the *SOI2* mutations nor *soi3-1* suppressed deletion of the C-tail, suggesting initially that both suppress through TLS1, i.e., by improving retrieval from the PVC back to the TGN. However, further analysis of the *soi3* null mutant, detailed in this work, showed that Soi3p functions in a distinct transport step important to Kex2p localization, between the early and late endosome.

Phenotypic analysis revealed that hypersensitivity to both Zn^{2+} and Co^{2+} cosegregated with the suppressor phenotype caused by the *soi3-1* mutation (our unpublished data). Wild-type *SOI3* was cloned from a yeast genomic library by complementing the Zn^{2+} hypersensitivity. Two clones

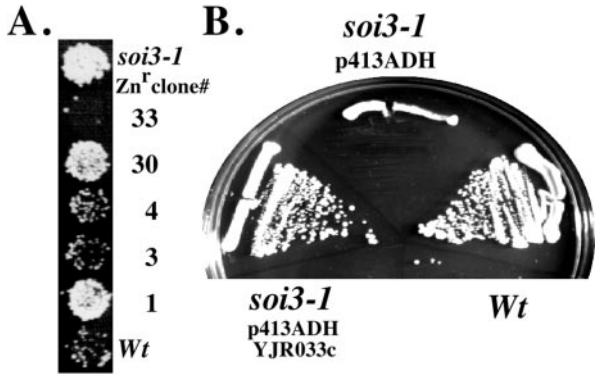

Figure 2. Cloning of *SOI3.* Zn^{2+}-resistant (Zn^r) clones were isolated by transforming SPB400-3D (*soi3-1*) cells carrying pCWKX10 with a yeast *CEN ARS* genomic library. (A) After the pCWKX10 plasmid was replaced with pCWKX21, Zn^r clones were tested for the ability to revert the Soi$^+$ phenotype to wild-type. Clones 3 and 4 were able to complement the Soi$^+$ phenotype and both contained the full-length YJR033c ORF. (B) Expression of YJR033c complemented *soi3-1* zinc hypersensitivity. Strains SPB400-r8 (*soi3-1*) containing pCWKX10 and pADH-YJR033c, SPB400-r8 containing pCWKX10 and vector p413ADH and KRY18-1A (*SOI3*) containing pCWKX10 were streaked on a YPAD plate containing 5 mM $ZnCl_2$.

(clones 3 and 4) (Figure 2A) contained overlapping inserts, complemented the suppressor phenotype, and were shown by segregation analysis to map to the *soi3-1* locus (see MATERIALS AND METHODS). A single yeast open reading frame from this locus, YJR033c, when placed under control of the moderate *ADH* promoter in the single copy *CEN* plasmid pADH-YJR033c (see MATERIALS AND METHODS), complemented both the Zn^{2+} hypersensitivity (Figure 2B) and Soi$^+$ suppressor phenotypes of *soi3-1* (our unpublished data), confirming the identity of YJR033c as *SOI3.* As described previously (Kraemer *et al.*, 1998; Seol *et al.*, 2001), YJR033c encodes a large protein (~150 kDa) homologous to the DmX protein of *Drosophila melanogaster* and the human homolog DMXL1 2000) (Kraemer *et al.*, 1998; Kraemer *et al.*, 2000). Soi3p, approximately one-half the size of the metazoan homologues, is predicted to contain at least seven WD40 repeat sequences (Smith *et al.*, 1999), whereas DmX and DMLX1 may contain 28–30 WD repeats (Kraemer *et al.*, 2000). The carboxy terminus of the Soi3p sequence suggests the presence of a coiled-coil domain (residues 1311–1340). Soi3p is identical to Rav1p, which was isolated as a Skp1p–interacting protein implicated in assembly of vacuolar ATPase (V-ATPase) (Seol *et al.*, 2001). This work focuses on the role of Soi3/Rav1p in early endosome to PVC transport, but implicit in this is the expectation that it is the role of the protein in V-ATPase assembly at the early endosome that is key. Unpublished data from our laboratory along with published data support the conclusion that V-ATPase mutants have phenotypes similar to those exhibited by *soi3* mutants (our unpublished data) (Perzov *et al.*, 2002). Because *soi3-1* was described earlier than *RAV1* (Redding *et al.*, 1996a; Seol *et al.*, 2001), *SOI3* and Soi3p will be used here except where identity between Soi3p with Rav1p needs emphasis.

soi3-1 *Accumulates Early Endosome-like Structures*

Electron microscopic analysis of the *soi3-1* mutant was conducted using thick sections (250 nm) analyzed at tilt angles to permit creation of stereo pairs (Rambourg *et al.*, 1993). The *soi3-1* mutant cells massively accumulated ovoid membrane

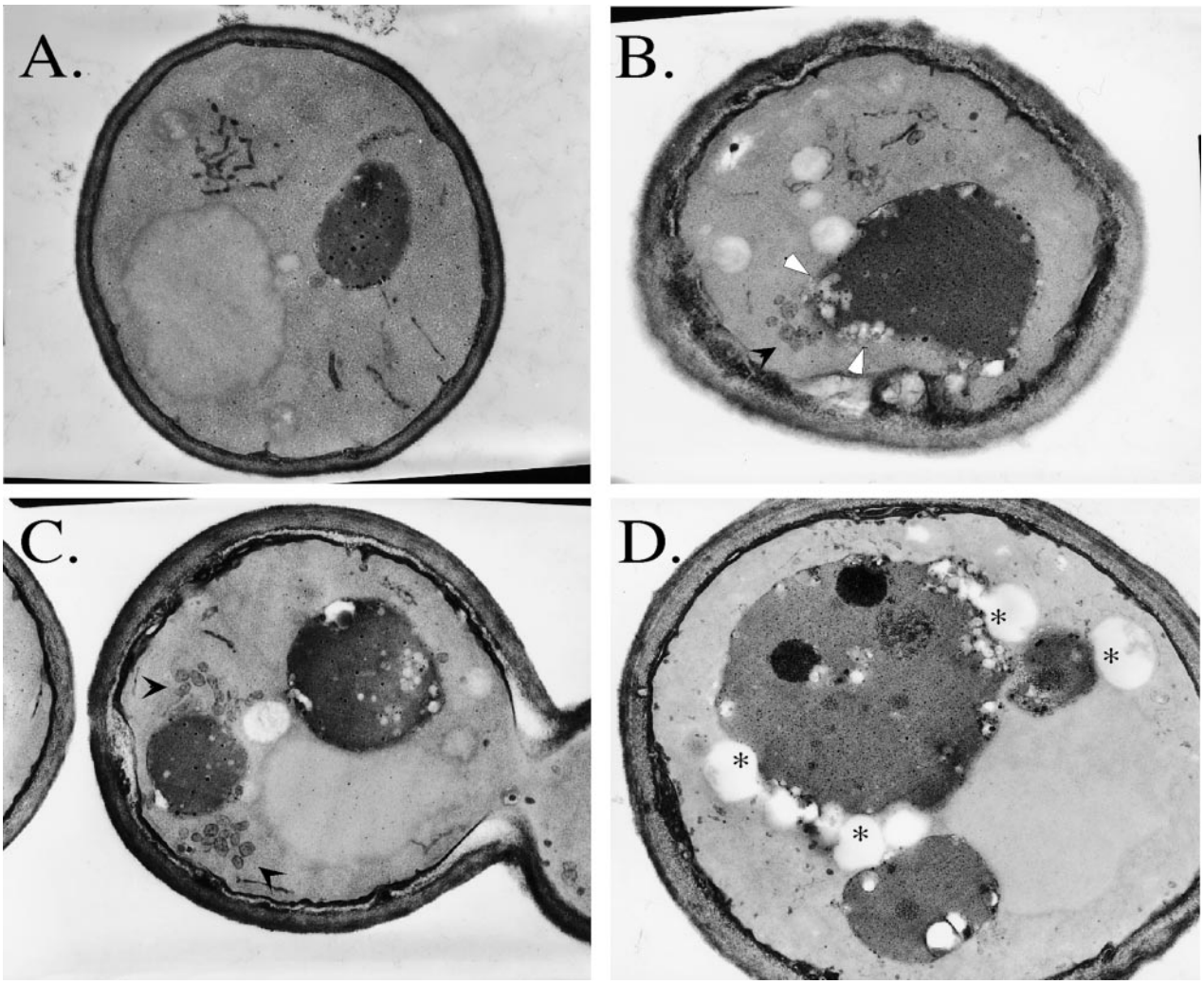

Figure 3. Aberrant organelles accumulate in *soi3-1* cells. Electron microscopy of wild-type (CRY2) (A) and *soi3-1* (SPB400-r8) cells (B–D). Black arrowheads indicate the accumulation of fenestrated ovoids (endosome-like structures, B and C) and white arrowheads point to ovoids contiguous with and apparently fusing with vacuoles (B). Asterisks label excess lipid particles also seen in *soi3-1* mutants (D).

structures that consisted of clusters of basket-like structures formed from anastomosed tubules (Figure 3). Clusters occurred near the vacuole or facing finger-like invaginations of the plasma membrane, suggestive in appearance of early endosomal tubulo-vesicular structures shown to label with positively charged nanogold (Prescianotto-Baschong and Riezman, 1998). These structures, which might be aberrant early or late endosomes, also were found adjacent to the vacuole, and, in some cases, seemed to be fusing with vacuoles (Figure 3, B and C). These structures were distinct from probable lipid particles, which also seemed to accumulate in the *soi3-1* mutant (Figure 3D).

soi3Δ *Causes a Kinetic Delay in Endocytic Delivery of FM4-64 to the Vacuole*

To assess the effects of loss of Soi3p function on bulk-phase endocytosis, *soi3*Δ cells were stained, on ice, with the lipophilic fluorescent dye FM4-64, warmed to 14°C, and then treated with sodium azide and sodium fluoride to deplete ATP (Figure 4). At 14°C, FM4-64 was found to accumulate in peripheral, punctate, endocytic structures in both wild-type and *soi3*Δ strains, as has been observed previously for cells maintained at 15°C (Vida and Emr, 1995). When cells were then shifted to 30°C for 5 min, FM4-64 chased to the vacuolar membrane in wild-type cells but persisted in punctate structures in *soi3*Δ cells. Extensive vacuolar membrane staining was observed in the *soi3*Δ cells after 30 min at 30°C, although persistent staining of one or two extravacuolar punctate structures was still apparent (Figure 4). No delay was observed in internalization of FM4-64 from the plasma membrane to internal sites when cells stained on ice were warmed to 30°C (our unpublished data), suggesting that loss of Soi3p results in a decreased rate of trafficking from an early endocytic intermediate to the vacuole.

The soi3Δ *Mutant Is Defective in Constitutive Vacuolar Degradation of Ste3p but Not Defective in Internalization or Endocytic Recycling of Ste3p.*

The **a**-factor receptor, Ste3p, undergoes endocytic internalization followed by delivery to the vacuole and degradation. Internalization occurs by two pathways. Constitutive internalization, which occurs in the absence of ligand, depends on ubiquitination within a PEST sequence in the C-terminal cytosoplasmic tail domain of Ste3p and results in a 20-min

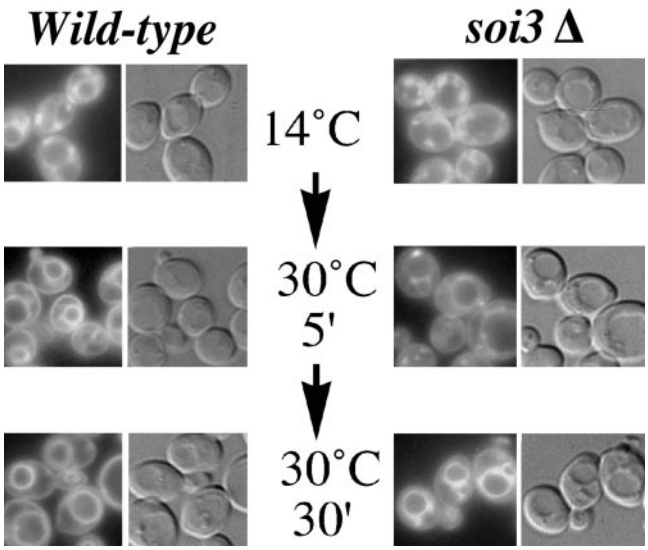

Figure 4. *soi3*Δ cells exhibit a kinetic delay in the uptake of FM 4-64 to the vacuole. Cells were preincubated with FM4-64 on ice, washed, and shifted to 14°C for 40 min to allow uptake in the 14°C early endosomal compartment. Cells were shifted to 30°C and at 5 or 30 min, treated with sodium azide plus fluoride, and visualized by fluorescence microscopy. The difference in plasma membrane staining between the wild-type and *soi3*Δ strains seen at 5 min in the figure was not a reproducible observation (our unpublished data). Strains were: GSY11–2A (*soi3*Δ) and GSY11-4D (wild type).

$t_{1/2}$ (Roth and Davis, 1996). Deletion of this PEST region by truncation of 105 residues of the C-terminal domain results in persistence of receptor at the plasma membrane. The truncated receptor, Ste3Δ365p, however, can be induced to undergo internalization by addition of **a**-factor. Ligand-dependent internalization of Ste3Δ365p leads to its recycling to the cell surface and slow vacuolar degradation. The effect of the *soi3*Δ mutation on each of these three pathways of Ste3p metabolism, constitutive endocytosis, ligand-dependent vacuolar turnover, and recycling to the plasma membrane was examined (Figure 5, A–D). Constitutive vacuolar degradation of Ste3p was found to occur with a $t_{1/2}$ of 27 min in the WT background. Ste3p was clearly stabilized in the *soi3*Δ strain, exhibiting a $t_{1/2}$ of 40 min (Figure 5A), indicating that vacuolar delivery by the constitutive internalization pathway was impaired. In contrast, a *soi1*Δ strain exhibited kinetics of constitutive vacuolar turnover of Ste3p indistinguishable from wild-type (our unpublished data).

Ligand-dependent turnover of Ste3Δ365p occurs, after a lag, with a $t_{1/2}$ of ~80 min (Chen and Davis, 2000). Ligand-induced turnover was only slightly slower in the mutant background, as evident by the persistence of a higher level of receptor in the mutant at 2 h after addition of **a**-factor (Figure 5B). Kinetics of ligand-induced internalization of the truncated receptor, as measured by protease shaving, however, were indistinguishable in the wild-type and *soi3*Δ strains (Figure 5C). Finally, kinetics of receptor recycling, as measured by sensitivity of receptor to external protease at times after removal of **a**-factor, were indistinguishable in the wild-type and mutant strains (Figure 5D). The fact that ligand-induced internalization and recycling rates were unchanged but that the overall rate of degradation of Ste3Δ365p was slowed suggests that transport from an endocytic compartment to the vacuole is delayed in the *soi3*Δ mutant strain.

The soi3Δ *Mutant Is Not Defective in* Zn^{2+}*-induced Vacuolar Degradation of Zrt1p*

To extend the analysis of loss of Soi3p function to other internalization events, we examined the Zn^{2+}-induced internalization of the high-affinity Zn^{2+} transporter Zrt1p (Gitan *et al*., 1998; Gitan and Eide, 2000). Expression of Zrt1p was extremely low in the *soi3*Δ strain relative to wild-type (data not shown). We hypothesized that *soi3*Δ strains have a higher constitutive concentration of free Zn^{2+} in the cytosol, resulting in repression of Zrt1p synthesis (Bird *et al*., 2000). To express Zrt1p in *soi3*Δ and wild-type strains at comparable levels, cells expressing an epitope-tagged form of Zrt1p (Zrt1-HAp) under the *ZRT1* promoter were grown in the presence of 1 mM EDTA for 3 h to lower Zn^{2+} availability and induce synthesis of Zrt1-HAp. $ZnCl_2$ was then added to 2 mM to shut off expression of *ZRT1-HA* and initiate down-regulation of the transporter (Gitan *et al*., 1998). In contrast to the results observed with Ste3p, rates of degradation of Zrt1-HAp were identical in the wild-type and *soi3*Δ cells (Figure 5E).

Soi3p Is a Peripheral Membrane Protein Associated with a High-density Membrane Compartment

Soi3p was tagged at the C-terminus with a triple HA-epitope tag (Soi3-HA3p). Differential centrifugation of crude lysates established that the protein was distributed between a soluble form and a form that sedimented at 200,000 × *g* (Figure 6A). The distribution between soluble and membrane-bound pools varied from experiment to experiment. The sedimentable form was released into the soluble fraction by treatment with 1.0 M NaCl, consistent with the behavior of Soi3p as a peripheral membrane protein (Figure 6A). When membranes containing Soi3-HA3p were subjected to sucrose equilibrium density gradient fractionation, Soi3-HA3p was found in high-density fractions (Figure 6B). The distribution of Soi3-HA3p was distinct from that of the Golgi GDPase, the PVC t-SNARE Pep12p, and the bulk of the TGN-marker protein Kex2p (Sipos and Fuller, 2002), although each of these proteins was present in small amounts in the dense fractions containing Soi3-HA3p (Figure 6B). Soi1p/Vps13p, also a peripheral membrane protein, labeled with the same epitope tag, also fractionated in a broader distribution than Soi3-HA3p (Figure 6B), consistent with proposed roles at the TGN and PVC (Brickner and Fuller, 1997). The high density of Soi3p membranes is suggestive of early endocytic membranes, because studies of α-factor internalization demonstrated a higher density for early versus late endocytic carriers (Singer-Kruger *et al*., 1993). Additionally, Soi3p cofractionated with the dense fraction of Chs3p, which is thought to reside in early endosomal membranes (Figure 6B) (Valdivia *et al*., 2002). These results suggest that Soi3p associates with early endosomes rather than TGN or late endosomes. Despite the fact that a fraction of Soi3-HA3p associates with membranes, as shown by sucrose gradient fractionation, the protein still sedimented in the P200 fraction in the presence of 1% Triton X-100 (Figure 6A). This, together with the fact that 1.0 M NaCl completely extracted the protein from the P200, implies that Soi3-HA3p that sediments in the P200 fraction represents a membrane-associated high-molecular weight, salt-sensitive complex. Consistent with the association of a fraction of Soi3p with a membrane compartment, Soi3-GFP exhibited a punctate pattern of fluorescence superimposed on a diffuse, cytosolic background (Figure 6C). Seol *et al*. (2001) previously detected only a diffuse, cytosolic distribution of Rav1p. The faint punctate pattern seen in Figure 6C has been enhanced

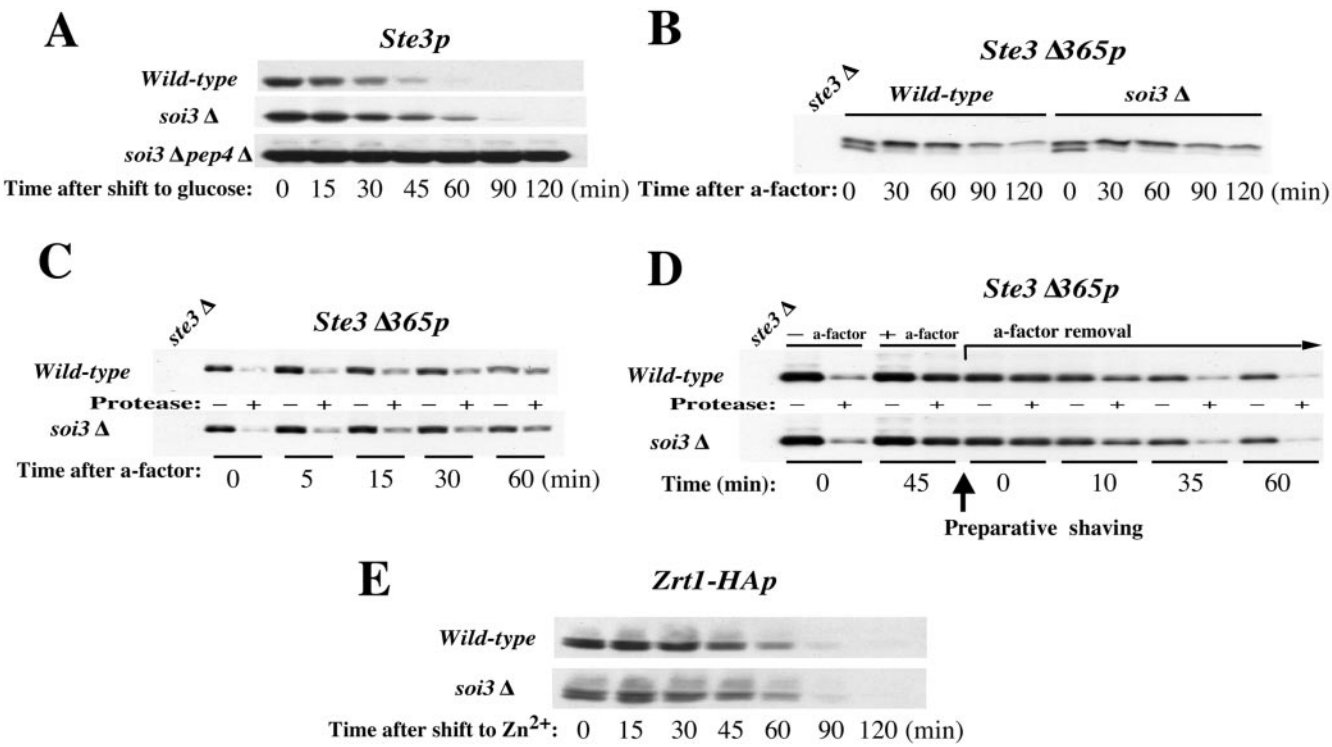

Figure 5. Turnover of Ste3p, Ste3Δ365p, and Zrt1HAp in *soi3*Δ cells. (A) Constitutive turnover of Ste3p. Ste3p expression was induced with galactose and terminated by the addition of glucose. (B) Ligand-induced turnover of Ste3Δ365p. After induction with galactose followed by a glucose chase (30 min), endocytosis was initiated by addition of **a**-factor. (C) Internalization assay for Ste3Δ365p. During ligand-dependent endocytosis, the level of internalized Ste3Δ365p was followed by a protease protection assay. (D) Recycling assay for Ste3Δ365p. After internalization was induced by adding **a**-factor, recycling of Ste3Δ365p to the cell surface was monitored by protease shaving after removal of the **a**-factor. (A–D) Strains containing *GAL1* promoter-driven *STE3* and *STE3*Δ*365* genes were GSY32 (*GAL1-STE3*), GSY34 (*GAL1-STE3 soi3*Δ), GSY36 (*GAL1-STE3 soi3*Δ *pep4*Δ), GSY40 (*GAL1-STE3*Δ*365*), and GSY41 (*GAL1-STE3*Δ*365 soi3*Δ). The *ste3*Δ control was GSY51. (E) Zn^{2+}-induced constitutive endocytosis of Zrt1HAp. Zrt1-HAp expression from pMC5-HSET in strains GSY11-4D (wild-type) and GSY11-2A (*soi3*Δ) was induced by 1 mM EDTA for 3 h, and turnover was initiated by adding fresh media containing 2 mM $ZnCl_2$. (A–E) Protein turnover was monitored by immunoblotting by using anti-HA (12CA5) and affinity-purified anti-Ste3p antibodies.

by image deconvolution (see MATERIALS AND METHODS), but it is observable without such enhancement. It is possible that some Soi3p may be associated with PVC membranes; however, consistent with localization of Soi3p to the early endosome rather than the PVC, we found that the pattern of Soi3-GFP localization was not altered by a class E *vps* mutation (*vps27*Δ), which typically causes late endosomal proteins to collapse to a single "class E spot" (our unpublished data) (Piper *et al*., 1995).

The soi3Δ *Strain Is Not Defective for Vacuolar Transport of proCPY, proALP, or proAPI*

Whereas *soi1* mutants exhibited a vacuolar protein sorting (Vps^-) defect (*SOI1* is allelic with *VPS13*) (Brickner and Fuller, 1997), neither *soi3-1* nor *soi3*Δ cells exhibited a Vps^- phenotype as judged by a colony-immunoblotting assay (Figure 7A). To determine whether loss of Soi3p function led to any discernible defect in delivery of newly synthesized proteins to the vacuole, cells were pulse-labeled with ^{35}S-amino acids and chased for various times. Lysates were subjected to immunoprecipitation with anti-carboxypeptidase Y antibodies to assess the Vps10p-dependent vacuolar transport pathway (Stevens *et al*., 1982; Klionsky and Emr, 1989), anti-ALP antibodies to assess the AP3-dependent pathway (Klionsky and Emr, 1989), and anti-API antibodies to assess the cytosol-to-vacuole (CVT) pathway (Klionsky *et al*., 1992). No difference was observed between the wild-type and *soi3*Δ mutant strains in the rate of delivery of proCPY to the vacuole, as judged by the rate of conversion of the Golgi form of proCPY (p2-CPY) to the mature form (m-CPY form; Figure 7B). Similarly, no alteration in the rate of delivery of proALP to the vacuole was observed in the *soi3*Δ mutant (Figure 7C). These results demonstrate that Soi3p does not play an essential role in either the Vps10p-dependent or AP3-dependent pathways from the Golgi to the vacuole. Finally, the rate of Ape1p maturation also was unaltered by the *soi3*Δ mutation (Figure 7D), indicating that the CVT pathway functions normally in the absence of Soi3p.

Soi3p *Functions Upstream from the Class E/PVC Compartment*

The *soi3-1* mutation was isolated because it suppressed the effects of the $Y_{713}A$ mutation in the TLS1 of Kex2p as measured by the efficiency of localization of the enzyme to the pro-α-factor processing compartment (Redding *et al*., 1996a). The *soi3-1* mutation was classified as an allele-specific suppressor in that it suppressed the effects of the $Y_{713}A$ mutation in TLS1 but not the effects of a complete deletion of the cytosolic tail (Redding *et al*., 1996a). The *soi3-1* mutation also suppressed the effects of the $F_{85}A$ mutation within the TGN localization signal in the N-terminal cytosolic tail of the Ste13p DPAPase A-ALP (Nothwehr *et al*., 1993; Redding *et al*., 1996a), suggesting that Soi3p function affects multiple TGN transmembrane proteins (Redding *et al*., 1996a).

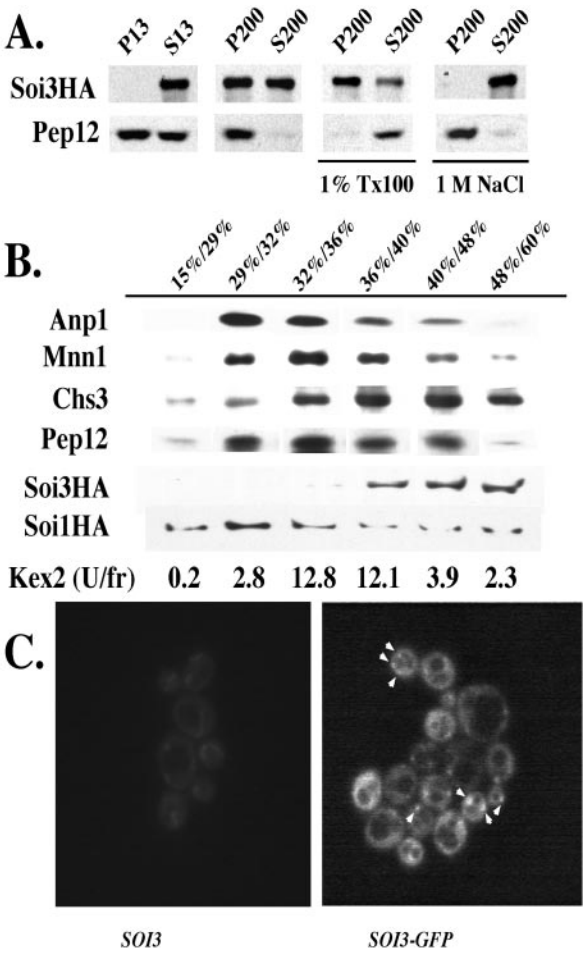

Figure 6. Localization of Soi3p by subcellular fractionation and fluorescence microscopy. (A) Spheroplast lysate of GSY11-2A expressing Soi3HAp from its own promoter on plasmid p*SOI3-HA* was fractionated as described in MATERIALS AND METHODS. Soi3HAp and Pep12p were probed by immunoblotting. (B) Spheroplast lysates were subjected to sucrose gradient fractionation as described in MATERIALS AND METHODS, and aliquots were tested for the distribution of Soi3HAp, Soi1Hap, and for Golgi and endosomal markers by immunoblotting and for the distribution of Kex2 proteolytic activity (Sipos and Fuller, 2002). Soi3HAp and all other markers except Soi1HAp were analyzed by fractionating lysates of GSY11-2A expressing Soi3HAp from the *ADH* promoter on plasmid p413ADH-*SOI3-HA*. Soi1HAp fractionation was followed in lysates from JBY142. (C) GSY11-1A cells (*soi3*Δ) containing control plasmid p413ADH-*SOI3* (left) or p413ADH-*SOI3*-GFP (right) were examined by fluorescence microscopy and image deconvolution. Z-stacks of logarithmically grown cells were captured and processed using ISEE deconvolution software to enhance the punctate signal. In the right panel, arrowheads point to punctate structures that occur against a background of cytosolic Soi3-GFP fluorescence. The left panel shows an identical exposure of the control strain. Image deconvolution of Z-stacks of cells expressing soluble GFP under *ADH* promoter control revealed no punctate structures (our unpublished data).

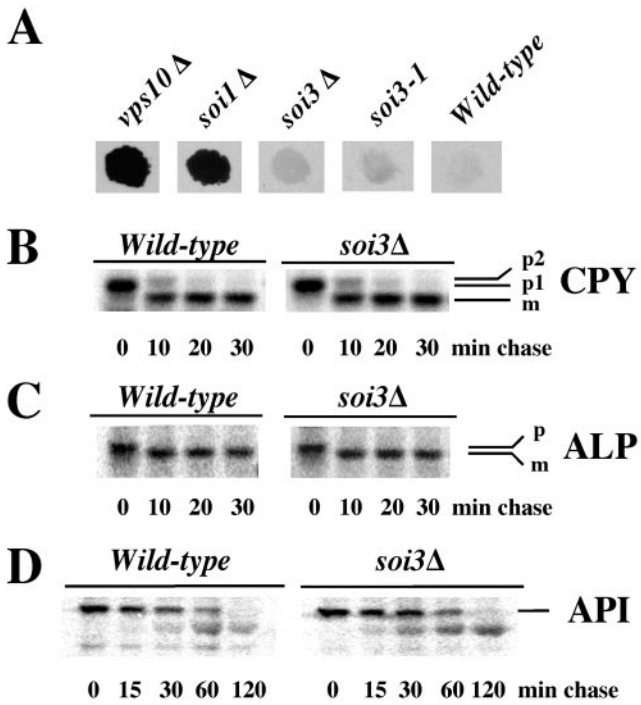

Figure 7. Mutation of *SOI3* does not affect the CPY, ALP, or CVT pathways. (A) Vacuolar protein sorting defects were assayed by detecting secreted vacuolar protease CPY. Cells were grown on a nitrocellulose filter on a YPAD plate for 2 d, and the filters washed and immunoblotted for secreted CPY. Strains were GSY19 (*vps10*Δ), JBY135-1A (*soi1*Δ), GSY11-2A (*soi3*Δ), SPB400-3D (*soi3-1*), and GSY11-4D (wild type). (B–D) Kinetics of processing of proCPY (B), proALP (C), and proAPI (D) in wild-type (GSY11-4D) and *soi3*Δ (GSY11-2A) cells were determined by ^{35}S pulse-chase/immunoprecipitation as described in MATERIALS AND METHODS.

These results suggested that the *soi3-1* mutation might suppress the effects of TLS1 mutations by restoring retrieval of TLS1 mutant proteins from the late endosome. However, the effects of *soi3* mutations on endocytic delivery to the vacuole and the fractionation properties of Soi3-HA3p suggested the alternative possibility that Soi3p governs the sorting of Kex2p and Ste13p through an early endosomal compartment. If this were so, Soi3p should function upstream of the late endosome, a role that could be tested by examining the epistasis of *soi3* and a class E *vps* mutation. The class E *vps* mutation *vps27* interferes with the function of the late endosome, blocking both transport to the vacuole and retrieval to the TGN (Piper *et al*., 1995). Vacuolar proteases become active in the aberrant late endosome, resulting in the degradation of TGN membrane proteins that cycle through that compartment. Mutations in TLS1 do not alter the half-life of Kex2p or A-ALP in a class E *vps* mutant strain, consistent with the function of TLS1 in retrieval from the late endosome (Brickner and Fuller, 1997; Bryant and Stevens, 1997). In contrast, the presence of TLS2 was found to delay degradation of Kex2p and Ste13p in such a strain, consistent with it acting upstream from the late endosome, formally as a "TGN retention" signal (Brickner and Fuller, 1997; Bryant and Stevens, 1997).

To test epistasis of *soi3*Δ and *vps27*Δ, *vps27*Δ and *vps27*Δ *soi3*Δ strains were transformed with a *CEN* plasmid encoding a form of Kex2p, I718-tail-Kex2p, which contains TLS1 but not TLS2 (Brickner and Fuller, 1997). Pulse-chase immunoprecipitation demonstrated that whereas I718tail-Kex2p turned over rapidly ($t_{1/2}$ ~18 min; Table 2) in the *vps27*Δ strain (Figure 8A), the protein was stabilized in the *vps27*Δ *soi3*Δ double mutant ($t_{1/2}$ ~62 min; Figure 8A and Table 2). Y_{713}A-Kex2p, which has TLS2 but lacks TLS1, turned over more slowly in the *vps27*Δ strain ($t_{1/2}$ ~39 min; Table 2) but was still stabilized in the double mutant ($t_{1/2}$ ~93 min; Table 2). The *soi3*Δ mutation also delayed delivery of WT Kex2p to

Table 2. Half-lives (minutes) of wild-type and C-tail mutant forms of Kex2p in wild-type and mutant backgrounds

Form of Kex2p	WT	*soi3-1*	*soi3*-Δ	*soi3*Δ*vps27*Δ	*vps27*Δ
WT	79	150	62	92	36
Y713A	20	36	41	93	39
I718tail	80	79	84	62	18
C-tailΔ	10	10	20	ND	ND

ND, not determined.

the class E compartment in the *vps27*Δ background (Table 2). These data argue strongly that the effect of the *soi3*Δ mutation on Kex2p occurs upstream from the late endosome.

Vps10p Endosomal Cycling Does Not Require Soi3p

The observation that proCPY sorting was not affected by loss of Soi3p function implied that the *soi3*Δ mutation should not affect cycling of the Vps10p receptor. This was confirmed by examining the fate of Vps10p by pulse-chase/immunoprecipitation in *vps27*Δ and *vps27*Δ *soi3*Δ strains. Vps10p undergoes proteolytic clipping when delivered to the aberrant late endosome in a *vps27*Δ strain (Figure 8B) (Bryant and Stevens, 1997). In contrast to the stabilization of Kex2p, the rate and extent of proteolytic clipping of Vps10p were not altered by the *soi3*Δ mutation (Figure 8B). These results rule out the possibility that the *soi3*Δ merely abrogates proteolytic activity in the class E compartment, because proteolytic cleavage of Vps10p was identical in the *vps27*Δ and *vps27*Δ *soi3*Δ strains. Therefore, we conclude that loss of Soi3p function interferes with a pathway traveled by Kex2p and not by Vps10p.

soi3Δ *and* **soi3-1** *Have Different Effects on Wild-Type, $Y_{713}A$, and C-tail***Δ***-Kex2p*

The *soi3-1* mutation was classified as an allele-specific suppressor of the $Y_{713}A$ mutation in the Kex2p cytosolic tail because it failed to suppress, in the onset of impotence assay, the effects of either the complete deletion of the tail (C-tailΔ) or deletion of roughly 30 residues in the membrane proximal

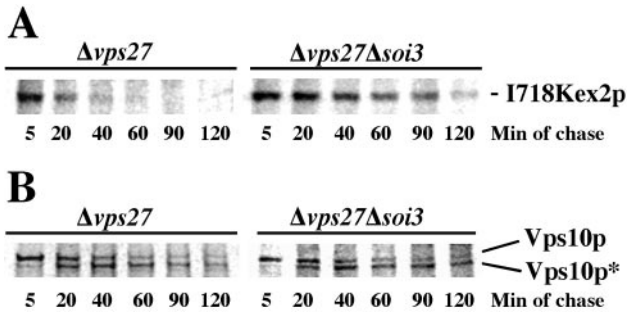

Figure 8. Deletion of *SOI3* prevents the rapid turnover of I718Kex2p in *vps27*Δ cells. EBY22 (*soi3*Δ *kex2*Δ *vps27*Δ) cells carrying pCWKX10-I718 and either pRS413ADH-*SOI3* (*vps27*Δ) or pRS413ADH (*vps27*Δ *soi3*Δ) were subjected to ^{35}S pulse-chase/immunoprecipitation as described in MATERIALS AND METHODS. Vps10* refers to the clipped form of Vps10p produced by proteolysis of Vps10p by activated vacuolar proteases in the class E PVC compartment (Bryant and Stevens, 1997). Anti-lumenal antiserum was used for IP of I718Kex2p.

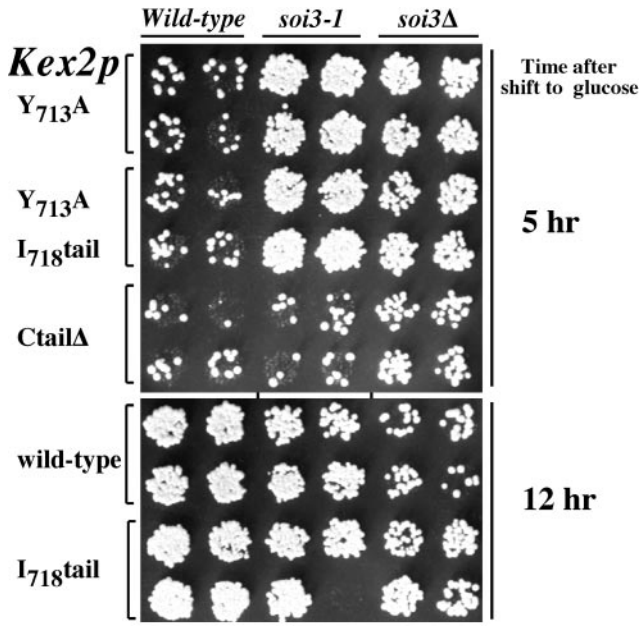

Figure 9. *soi3*Δ and *soi3-1* exert different effects in the onset of impotence assay. Strains KRY18–1A (*SOI3*), SPB400–3D (*soi3–1*) and GSY11–7A (*soi3*Δ) carrying plasmids pCWKX21 (*GAL-KEX2 $Y_{713}A$*), pCWKX21-I718 (*GAL-KEX2 $Y_{713}A$ I718tail*), pCWKX27 (*GAL-KEX2 C-tail*Δ), pCWKX20 (*GAL-KEX2*), pCWKX20-I718tail (*GAL-KEX2 I718tail*) were shifted from galactose to glucose medium for the indicated times and assessed for mating competence as described (Redding *et al*., 1996a).

portion of the tail that removed TLS1 (Redding *et al*., 1996a). The *soi3-1* mutation lengthened the half-life of both wild-type and $Y_{713}A$ Kex2p and was shown to be recessive for its effect on the half-life of $Y_{713}A$ Kex2p (Redding *et al*., 1996a). Surprisingly, the *soi3*Δ mutation had distinct effects. First, the deletion mutation suppressed both the $Y_{713}A$ and C-tailΔ mutations in the onset of impotence assay (Figure 9, top, top and bottom rows). Both the *soi3-1* and *soi3*Δ mutations suppressed the $Y_{713}A$ mutation in the absence of TLS2; that is, the $Y_{713}A$, I718tail-Kex2p was indistinguishable from $Y_{713}A$-Kex2p in this assay (Figure 9, top, middle rows). In addition, whereas the *soi3-1* mutation had no obvious effect on wild-type Kex2p, the *soi3*Δ mutation had a negative effect on the persistence of the wild-type enzyme in the pro-α-factor processing compartment as judged by the onset of impotence assay (Figure 9, bottom, top two rows). This effect was not seen with I718tail Kex2p, which possesses TLS1 but lacks TLS2 (Figure 9, bottom, bottom two rows).

Pulse-chase analysis confirmed these observations (Figure 10; data summarized in Table 2). Whereas the *soi3-1* mutation slowed vacuolar turnover of wild-type Kex2p, the *soi3*Δ mutation accelerated it (Figure 10A and Table 2). In contrast, the *soi3*Δ slightly delayed transport of I718tail-Kex2p to the vacuole (Table 2). Both the *soi3-1* and *soi3*Δ mutations delayed vacuolar turnover of $Y_{713}A$-Kex2p (Figure 10B and Table 2). In agreement with the onset of impotence data, the *soi3*Δ delayed the vacuolar turnover of C-tailΔ-Kex2p, but the *soi3-1* mutation had no effect (Figure 10C and Table 2). Consistent with the different effects of *soi3-1* and *soi3*Δ mutations, *soi3-1* was found to correspond to a single nucleotide change (G to A at position 350 in the structural gene), resulting in substitution of Glu for Gly_{118} (our unpublished data).

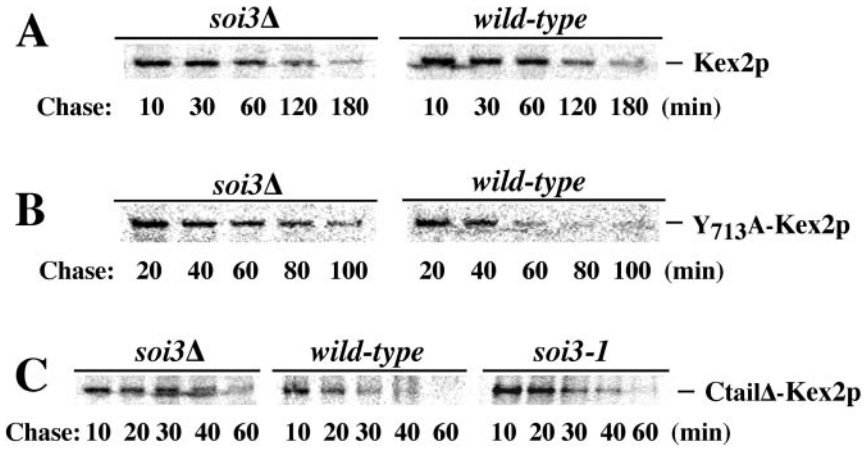

Figure 10. Effects of the *soi3* mutants on the turnover of C-tail mutant forms of Kex2p. GSY11-2A (*soi3*Δ), SPB400-3D (*soi3-1*), and GSY11-4D (wild type) cells carrying plasmids (A) pCWKX10 (WT Kex2p), (B) pCWKX11 (Y_{713}A-Kex2p), or (C) pCWKX17 (C-tailΔ-Kex2p) were subjected to ^{35}S pulse-chase/immunoprecipitation as described in MATERIALS AND METHODS. Anti-C-tail antiserum was used for IP of wild-type Kex2p and Y_{713}A-Kex2p, and anti-lumenal antiserum was used for IP of C-tailΔ-Kex2p.

SOI3 *and* VPS1 *Govern Distinct Pathways to the Vacuole*

The effect of the *soi3*Δ on endocytic cargo seemed to be selective, in that delivery of Ste3p to the vacuole was delayed but delivery of Zrt1p was not. In addition, loss of Soi3p did not completely block vacuolar delivery of either FM4-64 or Ste3p, suggesting the existence of one or more bypass pathways. One possible bypass pathway would be from the early endosome to the TGN and thence to the PVC. The difference between Ste3p and Zrt1p in the *soi3*Δ background might be due to transport of Zrt1p via such a pathway. In this case, mutation of *VPS1*, which is required for TGN to PVC transport (Wilsbach and Payne, 1993; Nothwehr *et al*., 1995) would be expected to interfere with endocytic transport of Zrt1p to the vacuole. When *VPS1* was deleted in a *soi3*Δ/*SOI3* heterozygous diploid and in a *soi3*Δ/*soi3*Δ homozygous diploid, tetrad analysis demonstrated synthetic lethality between *vps1*Δ and *soi3*Δ (our unpublished data). To determine the effect of loss of *VPS1* function on Zrt1p and Ste3p in a *soi3*Δ background, a strain was constructed that contained a temperature-sensitive allele of *VPS1* and the *soi3*Δ. When down-regulation of Zrt1HAp was induced by Zn^{2+} addition, vacuolar degradation of the protein was delayed in the *vps1-ts* strain relative to the wild-type strain even at the permissive temperature of 26°C (Figure 11A). Zrt1HAp degradation was accelerated in the wild-type strain at 37°C relative to 26°C (Figure 11A). In contrast, the presence of the *vps1-ts* allele strongly stabilized Zrt1HAp at 37°C (nonpermissive temperature the *vps1-ts* allele), and addition of the *soi3*Δ mutation did not augment this effect (Figure 11A). Ste3HAp behaved in the opposite manner. Although deletion of *SOI3* clearly stabilized Ste3HAp in the *vps1-ts* background both at 26 and 37°C, the *vps1-ts* mutation had no effect on the constitutive rate of Ste3HAp turnover in either the *SOI3* or *soi3*Δ background at either temperature (Figure 11B). Thus, whereas Zn^{2+}-induced down-regulation and vacuolar degradation of Zrt1HAp was Vps1p dependent and Soi3p independent, constitutive endocytic degradation of Ste3HAp was Soi3p dependent and Vps1p independent.

DISCUSSION

Soi3p Function Is Required for Early Endosome-to-PVC Transport

SOI3 was identified by a recessive allele, *soi3-1*, that suppressed vacuolar mislocalization of Y_{713}A-Kex2p as well as mutation of the TGN retrieval signal in the Ste13p cytosolic tail (Redding *et al*., 1996a). Unlike mutations in *SOI1/VPS13* (Brickner and Fuller, 1997), *soi3* mutations suppressed the Y_{713}A mutation in the absence of the TGN retention signal TLS2 (Figure 1B). The fact that the *soi3* mutations were recessive and had no defect in vacuolar protein sorting suggested that loss of Soi3p either improved retrieval of TLS1-mutant forms of Kex2p and Ste13p from the PVC or that a novel mechanism was at work.

The evidence presented here argues for a novel mechanism, that Soi3p functions at the early endosome and is important for transport of both endocytic cargo and TGN transmembrane proteins from the early endosome to the PVC. First, *soi3*Δ mutants exhibit a kinetic delay in delivery of FM4-64 to the vacuole, with the delay occurring in transport between the 14°C endocytic intermediate compartment and the vacuole. Consistent with the persistence of FM4-64 staining in punctate structures in the *soi3*Δ mutant, we observed accumulation of fenestrated, tubular membrane structures in the *soi3-1* mutant by EM. Second, the rate of

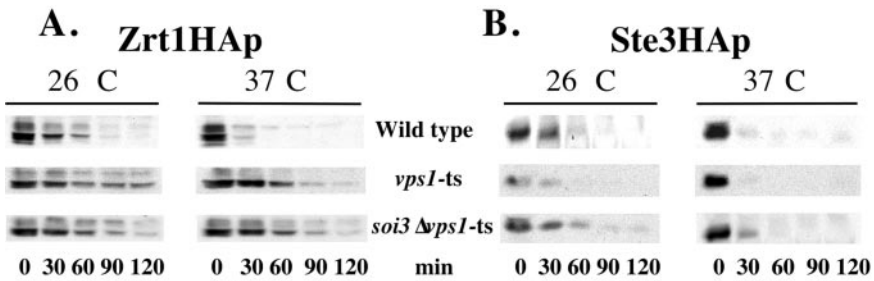

Figure 11. Differential effects of *soi3*Δ and *vps1-ts* mutations on Zrt1HAp and Ste3HAp. Zrt1HAp (A) and Ste3HAp (B) were expressed in wild-type (GSY11-4D), *vps1-100-ts* (EBY77-4) and *soi3*Δ *vps1-100-ts* (EBY77-8) cells. Zrt1HAp turnover was initiated as described in MATERIALS AND METHODS. Ste3HAp was induced from the *GAL1* promoter on galactose media, and its expression was turned off by the addition of glucose. Both proteins were induced in cells growing at 26°C. Cells were then harvested, and aliquots were diluted with fresh media prewarmed either to 26 or 37°C. Protein turnover was followed by immunoblotting.

constitutive vacuolar turnover of the Ste3p **a**-factor receptor was substantially decreased in the *soi3*Δ mutant, whereas rates of internalization and recycling of Ste3p were unaltered. Third, membrane-associated Soi3p cofractionated with Chs3p in a dense fraction characteristic of early endosomes. Consistent with early endosome localization, a fraction of Soi3-GFP localized in a peripheral, punctate pattern. Fourth, *soi3* mutations delayed delivery of Y_{713}A-Kex2p, but not Vps10p, to the class E (aberrant PVC) compartment. The Vps10p-dependent, AP3-dependent, and CVT vacuolar targeting pathways were unaffected by loss of Soi3p. Each of these pathways is likely to require normal TGN functioning, including the CVT pathway, which depends on the TGN SNAREs Tlg1p and Tlg2p (Reggiori *et al*., 2003). Finally, the synthetic lethality of *soi3*Δ with *vps1*Δ, by itself, is consistent with Soi3p having a role in endocytotic transport to the vacuole, given the synthetic lethality of *vps1* with *end4* mutations (Nothwehr *et al*., 1995; Conibear and Stevens, 2000). Together, these data argue strongly for Soi3p function in early endosome to PVC transport. We should emphasize here, however, that we cannot rule out, on the basis of these data, roles for Soi3p in other transport steps, in particular between the PVC and the vacuole.

The *soi3* null mutation only partially blocked FM4-64 trafficking to the vacuole and endocytic degradation of Ste3p, but such partial effects are in line with the effects of other mutants shown to affect vacuolar delivery of FM4-64 and Ste3p (Gerrard *et al*., 2000; Heese-Peck *et al*., 2002; Shaw *et al*., 2003). The partial block may be due to the existence of a bypass pathway, but the fact that the delayed vacuolar delivery of Ste3p (Figure 11B) and FM4-64 (our unpublished data) was not further impaired by a *vps1-ts* mutation argues against transport of Ste3p and FM4-64 to the vacuole via the TGN-PVC pathway. The bypass pathway might instead correspond to direct fusion of early endosomes with the vacuole, a phenomenon suggested by EM analysis of the *soi3-1* mutant (Figure 3B). In contrast, the *vps1-ts* mutation did and the *soi3*Δ did not affect endocytic degradation of Zrt1p (Figures 5E and 11A), suggesting that Ste3p and Zrt1p follow different pathways to the vacuole.

Zinc Sensitivity of soi3 *Mutants*

Zn^{2+} hypersensitivity of the *soi3* mutants initially led us to examine endocytosis of Zrt1p. However, although we found that vacuolar delivery of Zrt1p induced by Zn^{2+} was unaltered in the *soi3* mutant, expression of Zrt1p was markedly reduced in growth in standard synthetic growth medium (our unpublished data), suggesting that *soi3* mutations disrupt Zn^{2+} homeostasis, leading to higher cytosolic Zn^{2+} levels. The possibility that *soi3* mutants are defective in Zn^{2+} sequestration in the vacuole is supported by the finding that *ZRC1*, which encodes a Zn^{2+} transporter in the vacuolar membrane (MacDiarmid *et al*., 2002), was isolated as a double-copy suppressor in the initial cloning of the *soi3-1* mutation by complementation of the Zn^{2+}-hypersensitive phenotype (clones 1 and 30 in Figure 2A; other data not shown).

Kex2p and Ste13p Cycle through the Early Endosome

Evidence presented here that Soi3p functions at the early endosome along with the effects of *soi3* mutations on Y_{713}A-Kex2p and F_{85}A-A-ALP (Redding *et al*., 1996a) argue that both Kex2p and A-ALP (as surrogate for Ste13p) cycle through the early endosome. Other studies support this. First, Kex2p partially colocalizes with Chs5p, which in turn colocalizes with Chs3p, a protein whose localization to an internal punctate organelle termed the chitosome requires endocytosis (Santos and Snyder, 1997; Ziman *et al*., 1998). Second, localization of Kex2p to an early or recycling endosome also was suggested by colocalization of Kex2p with GFP-labeled Snc1p, the v-SNARE of secretory vesicles, to punctate internal sites presumed to be intermediates in the recycling of Snc1p from the plasma membrane to the TGN (Lewis *et al*., 2000; Ha *et al*., 2001). Third, mutations in *INP53*, which encodes a synaptojanin homolog, interfered with the function of the TLS2-like signal in A-ALP (Ha *et al*., 2001). Mutation of *INP53* accelerated vacuolar delivery not only of F_{85}A-A-ALP but also of Kex2p without affecting Vps10p. Like mutations in the β subunit of the clathrin adaptor complex AP-1, *inp53* mutations were found to result in synthetic growth defects when combined with double mutations in *GGA1* and *GGA2*, leading to the suggestion that Inp53p and AP-1 were required for a TLS2-dependent transport pathway between the TGN and early endosome (Ha *et al*., 2003). Whereas, *inp53* mutations increased the rate of vacuolar delivery of $TLS1^-$ $TLS2^+$ forms of Kex2p and A-ALP (Y_{713}A-Kex2p and F_{85}A-A-ALP), *soi3* mutations decreased the rate of transit to the vacuole of the $TLS1^-$ $TLS2^+$ proteins. This can be understood if Inp53p (and AP-1) function in delivery of Ste13p and Kex2p to the early endosome and Soi3p functions in transport from the early endosome to the PVC.

Partitioning of Kex2p between Two TGN-PVC Pathways

The effects of *soi3* mutations on Kex2p argue that Kex2p can follow a pathway from the TGN through the early endo-

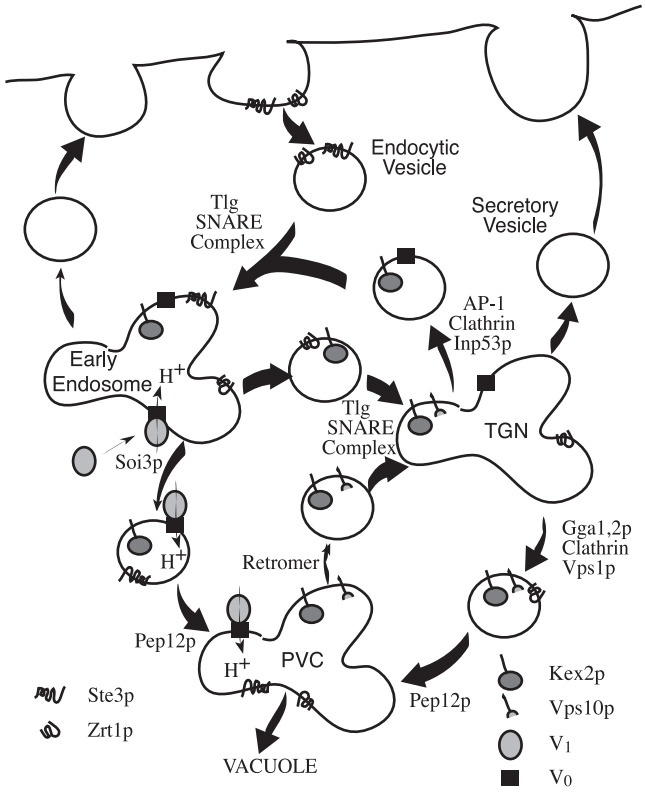

Figure 12. Model for TGN-endosomal transport pathways. The TGN-PVC pathway is depicted as requiring Gga proteins, clathrin and Vps1p. The TGN-early endosome pathway is depicted as requiring clathrin and Inp53p and involving fusion of endocytic vesicles with TGN derived vesicles in an event depending on the Tlg SNARE complex (Brickner *et al*., 2001). Soi3p is shown governing early endosome to PVC transport through V-ATPase assembly.

some to the PVC. However, the dramatic effects of *vps1* mutations on Kex2p localization (Wilsbach and Payne, 1993; Nothwehr *et al*., 1995) argue that Kex2p also partitions into the direct route between the TGN and PVC that is followed by Vps10p. TLS2, which is negatively regulated by Soi1/Vps13p (Brickner and Fuller, 1997), seems to influence this partitioning. In the class E *vps27* and *vps27 soi3*Δ backgrounds, the $TLS2^+$ wild-type and the Y_{713}A-forms of Kex2p behave identically. Both are stabilized by deletion of *SOI3*, consistent with these proteins partitioning identically between the two pathways. The $TLS2^-$ proteins I718tail-Kex2p and C-tailΔ-Kex2p are also both stabilized by the *soi3*Δ mutation in the *vps27* background, but to a lesser degree than the $TLS2^+$ proteins, suggesting that TLS2 is important for but not absolutely required for partitioning into the early endosome pathway.

The *soi3-1* allele exhibits Zn^{2+} and Co^{2+} sensitivity intermediate between that of wild-type *SOI3* and *soi3*Δ (our unpublished data) and therefore likely possesses residual function, although distinct effects of the *soi3*Δ and *soi3-1* alleles on Kex2p trafficking suggest that *soi3-1* may function as a "special" allele. Regardless, the effects of *soi3-1* and *soi3*Δ mutations on the half-life of the wild-type and C-tail mutant forms of Kex2p (Table 2 and Figure 10) correlate with their effects on Kex2p-dependent mating in the onset of impotence assay (Figure 9). For example, the *soi3-1* mutation increased the half-life of wild-type Kex2p and extended mating with wild-type Kex2p in the onset of impotence assay. The *soi3*Δ mutation slightly decreased both. One possibility is that an intermediate level function of Soi3-1p (e.g., resulting in reduced acidification of the early endosome; see below) enhances TLS1-dependent retrieval of wild-type Kex2p from the early endosome to the TGN.

V-ATPase Assembly and Early Endosome Maturation

Given the role of Soi3/Rav1p in V-ATPase assembly, the defect in early endosome to PVC transport seen in *soi3* mutants is presumably due to a failure in early endosome acidification. This is consistent with the finding that inhibition of V-ATPase in mammalian cells with bafilomycin A blocks early endosome maturation and results in accumulation of tubulo-vesicular compartments that resemble the structures accumulated in *soi3* mutants (Clague *et al*., 1994). This suggests a model wherein acidification of early endosomes in yeast, and possibly in mammalian cells, is regulated at the level of assembly of the V-ATPase. A curious point is that although Soi3/Rav1p is clearly required for efficient reassembly of V-ATPase at the vacuolar membrane (Seol *et al*., 2001; Smardon *et al*., 2002), Soi3p does not seem to be associated with vacuolar membranes. In particular, although Soi3-GFP is visualized as diffuse, cytosolic fluorescence along with faint punctate fluorescence, no vacuolar membrane fluorescence is observed (Figure 6B). One possibility is that Soi3p association with the vacuolar membrane is too transient to be detected, perhaps because it only occurs during regulated assembly of V-ATPase. An alternative possibility is that all V-ATPase assembly ordinarily occurs on endosomal vesicles followed by delivery to the vacuole. The mechanism by which the integral membrane component V_o might be delivered to endocytic vesicles is unclear, but it might occur by recycling from the vacuolar membrane (Bryant *et al*., 1998), conceivably via trafficking from the TGN. TGN-early endosome transport may be essential for early endosome formation and maturation precisely because it delivers V_o to endocytic vesicles. Soi3p is a Skp1p-associated protein that is apparently not part of an SCF E3 ubiquitin ligase (Seol *et al*., 2001). It is interesting that one other non-SCF-Skp1p–associated protein, Rcy1p, also is implicated in early endosome function, specifically in recycling to the cell surface (Galan *et al*., 2001). A model for TGN-endosomal cycling and the role of Soi3p in this pathway is presented in Figure 12.

ACKNOWLEDGMENTS

We are grateful to Drs. Nicholas Davis, David Eide, Scott Emr, Todd Graham, Jeanne Hirsch, Daniel Klionsky, Sean Munro, Randy Schekman, Tom Stevens, and members of the Fuller laboratory for generously providing reagents and antisera and for helpful discussions. This work was supported in part by National Institutes of Health grants GM-50915 and GM-39697 to R.S.F. and P30 CA46592 to the University of Michigan Comprehensive Cancer Center.

REFERENCES

Bird, A.J., Zhao, H., Luo, H., Jensen, L.T., Srinivasan, C., Evans-Galea, M., Winge, D.R., and Eide, D.J. (2000). A dual role for zinc fingers in both DNA binding and zinc sensing by the Zap1 transcriptional activator. EMBO J. *19*, 3704–3713.

Black, M.W., and Pelham, H.R. (2000). A selective transport route from Golgi to late endosomes that requires the yeast GGA proteins. J. Cell Biol. *151*, 587–600.

Black, M.W., and Pelham, H.R. (2001). Membrane traffic: how do GGAs fit in with the adaptors? Curr. Biol. *11*, R460–R462.

Brickner, J.H., Blanchette, J.M., Sipos, G., and Fuller, R.S. (2001). The Tlg SNARE complex is required for TGN homotypic fusion. J. Cell Biol. *155*, 969–978.

Brickner, J.H., and Fuller, R.S. (1997). SOI1 encodes a novel, conserved protein that promotes TGN-endosomal cycling of Kex2p and other membrane proteins by modulating the function of two TGN localization signals. J. Cell Biol. *139*, 23–36.

Bryant, N.J., Piper, R.C., Weisman, L.S., and Stevens, T.H. (1998). Retrograde traffic out of the yeast vacuole to the TGN occurs via the prevacuolar/endosomal compartment. J. Cell Biol. *142*, 651–663.

Bryant, N.J., and Stevens, T.H. (1997). Two separate signals act independently to localize a yeast late Golgi membrane protein through a combination of retrieval and retention. J. Cell Biol. *136*, 287–297.

Cereghino, J.L., Marcusson, E.G., and Emr, S.D. (1995). The cytoplasmic tail domain of the vacuolar protein sorting receptor Vps10p and a subset of VPS gene products regulate receptor stability, function, and localization. Mol. Biol. Cell *6*, 1089–1102.

Chen, L., and Davis, N.G. (2000). Recycling of the yeast a-factor receptor. J. Cell Biol. *151*, 731–738.

Chen, L., and Davis, N.G. (2002). Ubiquitin-independent entry into the yeast recycling pathway. Traffic *3*, 110–123.

Clague, M.J., Urbe, S., Aniento, F., and Gruenberg, J. (1994). Vacuolar ATPase activity is required for endosomal carrier vesicle formation. J. Biol. Chem. *269*, 21–24.

Conibear, E., and Stevens, T.H. (2000). Vps52p, Vps53p, and Vps54p form a novel multisubunit complex required for protein sorting at the yeast late Golgi. Mol. Biol. Cell *11*, 305–323.

Costaguta, G., Stefan, C.J., Bensen, E.S., Emr, S.D., and Payne, G.S. (2001). Yeast Gga coat proteins function with clathrin in Golgi to endosome transport. Mol. Biol. Cell *12*, 1885–1896.

Davis, N.G., Horecka, J.L., and Sprague, G.F., Jr. (1993). Cis- and trans-acting functions required for endocytosis of the yeast pheromone receptors. J. Cell Biol. *122*, 53–65.

Dell'Angelica, E.C., Puertollano, R., Mullins, C., Aguilar, R.C., Vargas, J.D., Hartnell, L.M., and Bonifacino, J.S. (2000). GGAs: a family of ADP ribosylation factor-binding proteins related to adaptors and associated with the Golgi complex. J. Cell Biol. *149*, 81–94.

Fuller, R.S., Sterne, R.E., and Thorner, J. (1988). Enzymes required for yeast prohormone processing. Annu. Rev. Physiol. *50*, 345–362.

Galan, J.M., Wiederkehr, A., Seol, J.H., Haguenauer-Tsapis, R., Deshaies, R.J., Riezman, H., and Peter, M. (2001). Skp1p and the F-box protein Rcy1p form a non-SCF complex involved in recycling of the SNARE Snc1p in yeast. Mol. Cell. Biol. *21*, 3105–3117.

Gerrard, S.R., Bryant, N.J., and Stevens, T.H. (2000). VPS21 controls entry of endocytosed and biosynthetic proteins into the yeast prevacuolar compartment. Mol. Biol. Cell *11*, 613–626.

Gitan, R.S., and Eide, D.J. (2000). Zinc-regulated ubiquitin conjugation signals endocytosis of the yeast ZRT1 zinc transporter. Biochem. J. *346*, 329–336.

Gitan, R.S., Luo, H., Rodgers, J., Broderius, M., and Eide, D. (1998). Zinc-induced inactivation of the yeast ZRT1 zinc transporter occurs through endocytosis and vacuolar degradation. J. Biol. Chem. *273*, 28617–28624.

Gueldener, U., Heinisch, J., Koehler, G.J., Voss, D., and Hegemann, J.H. (2002). A second set of loxP marker cassettes for Cre-mediated multiple gene knockouts in budding yeast. Nucleic Acids Res. *30*, e23.

Ha, S.A., Bunch, J.T., Hama, H., DeWald, D.B., and Nothwehr, S.F. (2001). A novel mechanism for localizing membrane proteins to yeast trans-Golgi network requires function of synaptojanin-like protein. Mol. Biol. Cell *12*, 3175–3190.

Ha, S.A., Torabinejad, J., DeWald, D.B., Wenk, M.R., Lucast, L., De Camilli, P., Newitt, R.A., Aebersold, R., and Nothwehr, S.F. (2003). The synaptojanin-like protein Inp53/Sjl3 functions with clathrin in a yeast TGN-to-endosome pathway distinct from the GGA protein-dependent pathway. Mol. Biol. Cell *14*, 1319–1333.

Heese-Peck, A., Pichler, H., Zanolari, B., Watanabe, R., Daum, G., and Riezman, H. (2002). Multiple functions of sterols in yeast endocytosis. Mol. Biol. Cell *13*, 2664–2680.

Hirst, J., Lui, W.W., Bright, N.A., Totty, N., Seaman, M.N., and Robinson, M.S. (2000). A family of proteins with gamma-adaptin and VHS domains that facilitate trafficking between the trans-Golgi network and the vacuole/lysosome. J. Cell Biol. *149*, 67–80.

Huang, K.M., D'Hondt, K., Riezman, H., and Lemmon, S.K. (1999). Clathrin functions in the absence of heterotetrameric adaptors and AP180-related proteins in yeast. EMBO J. *18*, 3897–3908.

Klionsky, D.J., Cueva, R., and Yaver, D.S. (1992). Aminopeptidase I of Saccharomyces cerevisiae is localized to the vacuole independent of the secretory pathway. J. Cell Biol. *119*, 287–299.

Klionsky, D.J., and Emr, S.D. (1989). Membrane protein sorting: biosynthesis, transport and processing of yeast vacuolar alkaline phosphatase. EMBO J *8*, 2241–2250.

Kolehmainen, J., *et al*. (2003). Cohen syndrome is caused by mutations in a novel gene, COH1, encoding a transmembrane protein with a presumed role in vesicle-mediated sorting and intracellular protein transport. Am. J. Hum. Genet. *72*, 1359–1369.

Kraemer, C., Enklaar, T., Zabel, B., and Schmidt, E.R. (2000). Mapping and structure of DMXL1, a human homologue of the DmX gene from *Drosophila melanogaster* coding for a WD repeat protein. Genomics *64*, 97–101.

Kraemer, C., Weil, B., Christmann, M., and Schmidt, E.R. (1998). The new gene DmX from *Drosophila melanogaster* encodes a novel WD-repeat protein. Gene *216*, 267–276.

Lewis, M.J., Nichols, B.J., Prescianotto-Baschong, C., Riezman, H., and Pelham, H.R. (2000). Specific retrieval of the exocytic SNARE Snc1p from early yeast endosomes. Mol. Biol. Cell *11*, 23–38.

MacDiarmid, C.W., Milanick, M.A., and Eide, D.J. (2002). Biochemical properties of vacuolar zinc transport systems of Saccharomyces cerevisiae. J. Biol. Chem. *277*, 39187–39194.

Mumberg, D., Muller, R., and Funk, M. (1995). Yeast vectors for the controlled expression of heterologous proteins in different genetic backgrounds. Gene *156*, 119–122.

Nothwehr, S.F., Conibear, E., and Stevens, T.H. (1995). Golgi and vacuolar membrane proteins reach the vacuole in vps1 mutant yeast cells via the plasma membrane. J. Cell Biol. *129*, 35–46.

Nothwehr, S.F., Roberts, C.J., and Stevens, T.H. (1993). Membrane protein retention in the yeast Golgi apparatus: dipeptidyl aminopeptidase A is retained by a cytoplasmic signal containing aromatic residues. J. Cell Biol. *121*, 1197–1209.

Perzov, N., Padler-Karavani, V., Nelson, H., and Nelson, N. (2002). Characterization of yeast V-ATPase mutants lacking Vph1p or Stv1p and the effect on endocytosis. J. Exp. Biol. *205*, 1209–1219.

Phan, H.L., Finlay, J.A., Chu, D.S., Tan, P.K., Kirchhausen, T., and Payne, G.S. (1994). The *Saccharomyces cerevisiae* APS1 gene encodes a homolog of the small subunit of the mammalian clathrin AP-1 complex: evidence for functional interaction with clathrin at the Golgi complex. EMBO J. *13*, 1706–1717.

Piper, R.C., Cooper, A.A., Yang, H., and Stevens, T.H. (1995). VPS27 controls vacuolar and endocytic traffic through a prevacuolar compartment in Saccharomyces cerevisiae. J. Cell Biol. *131*, 603–617.

Prescianotto-Baschong, C., and Riezman, H. (1998). Morphology of the yeast endocytic pathway. Mol. Biol. Cell *9*, 173–189.

Rambourg, A., Clermont, Y., and Kepes, F. (1993). Modulation of the Golgi apparatus in Saccharomyces cerevisiae sec7 mutants as seen by three-dimensional electron microscopy. Anat. Rec. *237*, 441–452.

Rampoldi, L., *et al*. (2001). A conserved sorting-associated protein is mutant in chorea-acanthocytosis. Nat Genet *28*, 119–120.

Redding, K., Brickner, J.H., Marschall, L.G., Nichols, J.W., and Fuller, R.S. (1996a). Allele-specific suppression of a defective trans-Golgi network (TGN) localization signal in Kex2p identifies three genes involved in localization of TGN transmembrane proteins. Mol. Cell. Biol. *16*, 6208–6217.

Redding, K., Holcomb, C., and Fuller, R.S. (1991). Immunolocalization of Kex2 protease identifies a putative late Golgi compartment in the yeast *Saccharomyces cerevisiae*. J. Cell Biol. *113*, 527–538.

Redding, K., Seeger, M., Payne, G.S., and Fuller, R.S. (1996b). The effects of clathrin inactivation on localization of Kex2 protease are independent of the TGN localization signal in the cytosolic tail of Kex2p. Mol. Biol. Cell *7*, 1667–1677.

Reggiori, F., Wang, C.W., Stromhaug, P.E., Shintani, T., and Klionsky, D.J. (2003). Vps51 is part of the yeast Vps fifty-three tethering complex essential for retrograde traffic from the early endosome and Cvt vesicle completion. J. Biol. Chem. *278*, 5009–5020.

Rose, M.D., Winston, F., and Heiter, P. (1990). Methods in Yeast Genetics: A Laboratory Course Manual, Cold Spring Harbor, NY: Cold Spring Harbor Laboratory Press.

Roth, A.F., and Davis, N.G. (1996). Ubiquitination of the yeast a-factor receptor. J. Cell Biol. *134*, 661–674.

Roth, A.F., Sullivan, D.M., and Davis, N.G. (1998). A large PEST-like sequence directs the ubiquitination, endocytosis, and vacuolar degradation of the yeast a-factor receptor. J. Cell Biol. *142*, 949–961.

Santos, B., and Snyder, M. (1997). Targeting of chitin synthase 3 to polarized growth sites in yeast requires Chs5p and Myo2p. J. Cell Biol. *136*, 95–110.

Seeger, M., and Payne, G.S. (1992). Selective and immediate effects of clathrin heavy chain mutations on Golgi membrane protein retention in *Saccharomyces cerevisiae*. J. Cell Biol. *118*, 531–540.

Seol, J.H., Shevchenko, A., and Deshaies, R.J. (2001). Skp1 forms multiple protein complexes, including RAVE, a regulator of V-ATPase assembly. Nat. Cell Biol. *3*, 384–391.

Shaw, J.D., Hama, H., Sohrabi, F., DeWald, D.B., and Wendland, B. (2003). PtdIns(3,5)P2 is required for delivery of endocytic cargo into the multivesicular body. Traffic *4*, 479–490.

Sikorski, R.S., and Hieter, P. (1989). A system of shuttle vectors and yeast host strains designed for efficient manipulation of DNA in *Saccharomyces cerevisiae*. Genetics *122*, 19–27.

Singer-Kruger, B., Frank, R., Crausaz, F., and Riezman, H. (1993). Partial purification and characterization of early and late endosomes from yeast. Identification of four novel proteins. J. Biol. Chem. *268*, 14376–14386.

Sipos, G., and Fuller, R.S. (2002). Separation of Golgi and endosomal compartments. Methods Enzymol. *351*, 351–365.

Smardon, A.M., Tarsio, M., and Kane, P.M. (2002). The RAVE complex is essential for stable assembly of the yeast V-ATPase. J. Biol. Chem. *277*, 13831–13839.

Smith, T.F., Gaitatzes, C., Saxena, K., and Neer, E.J. (1999). The WD repeat: a common architecture for diverse functions. Trends Biochem. Sci. *24*, 181–185.

Stepp, J.D., Pellicena-Palle, A., Hamilton, S., Kirchhausen, T., and Lemmon, S.K. (1995). A late Golgi sorting function for *Saccharomyces cerevisiae* Apm1p, but not for Apm2p, a second yeast clathrin AP medium chain-related protein. Mol. Biol. Cell *6*, 41–58.

Stevens, T., Esmon, B., and Schekman, R. (1982). Early stages in the yeast secretory pathway are required for transport of carboxypeptidase Y to the vacuole. Cell *30*, 439–448.

Tyers, M., Tokiwa, G., Nash, R., and Futcher, B. (1992). The Cln3-Cdc28 kinase complex of *S. cerevisiae* is regulated by proteolysis and phosphorylation. EMBO J. *11*, 1773–1784.

Ueno, S., Maruki, Y., Nakamura, M., Tomemori, Y., Kamae, K., Tanabe, H., Yamashita, Y., Matsuda, S., Kaneko, S., and Sano, A. (2001). The gene encoding a newly discovered protein, chorein, is mutated in chorea-acanthocytosis. Nat. Genet. *28*, 121–122.

Valdivia, R.H., Baggott, D., Chuang, J.S., and Schekman, R.W. (2002). The yeast clathrin adaptor protein complex 1 is required for the efficient retention of a subset of late Golgi membrane proteins. Dev. Cell *2*, 283–294.

Vida, T.A., and Emr, S.D. (1995). A new vital stain for visualizing vacuolar membrane dynamics and endocytosis in yeast. J. Cell Biol. *128*, 779–792.

Vida, T.A., Huyer, G., and Emr, S.D. (1993). Yeast vacuolar proenzymes are sorted in the late Golgi complex and transported to the vacuole via a prevacuolar endosome-like compartment. J. Cell Biol. *121*, 1245–1256.

Wach, A., Brachat, A., Pohlmann, R., and Philippsen, P. (1994). New heterologous modules for classical or PCR-based gene disruptions in *Saccharomyces cerevisiae*. Yeast *10*, 1793–1808.

Wilcox, C.A., and Fuller, R.S. (1991). Posttranslational processing of the prohormone-cleaving Kex2 protease in the *Saccharomyces cerevisiae* secretory pathway. J. Cell Biol. *115*, 297–307.

Wilcox, C.A., Redding, K., Wright, R., and Fuller, R.S. (1992). Mutation of a tyrosine localization signal in the cytosolic tail of yeast Kex2 protease disrupts Golgi retention and results in default transport to the vacuole. Mol. Biol. Cell *3*, 1353–1371.

Wilsbach, K., and Payne, G.S. (1993). Vps1p, a member of the dynamin GTPase family, is necessary for Golgi membrane protein retention in *Saccharomyces cerevisiae*. EMBO J. *12*, 3049–3059.

Yeung, B.G., Phan, H.L., and Payne, G.S. (1999). Adaptor complex-independent clathrin function in yeast. Mol. Biol. Cell *10*, 3643–3659.

Ziman, M., Chuang, J.S., Tsung, M., Hamamoto, S., and Schekman, R. (1998). Chs6p-dependent anterograde transport of Chs3p from the chitosome to the plasma membrane in Saccharomyces cerevisiae. Mol. Biol. Cell *9*, 1565–1576.